

Sample questions

- Describe the microbial loop and discuss its relevance for energy fluxes in a lake.
- Why would the relevance of allochthonous versus autochthonous energy sources to the aquatic metabolism change from small to large lakes?
- Describe the flood pulse concept and discuss its relevance for biodiversity across the aquatic-terrestrial continuum.
- What are the processes causing internal streambed clogging?

Ecosystem metabolism and restoration

The influence of floodplain restoration on whole-stream metabolism in an agricultural stream: insights from a 5-year continuous data set

Sarah S. Roley^{1,3}, Jennifer L. Tank^{1,4}, Natalie A. Griffiths^{1,5}, Robert O. Hall Jr.^{2,6}, and Robert T. Davis^{1,7}

Restoration and stream metabolism

- From an incised channel to a wider channel with floodplains
- Implications for hydraulic geometry

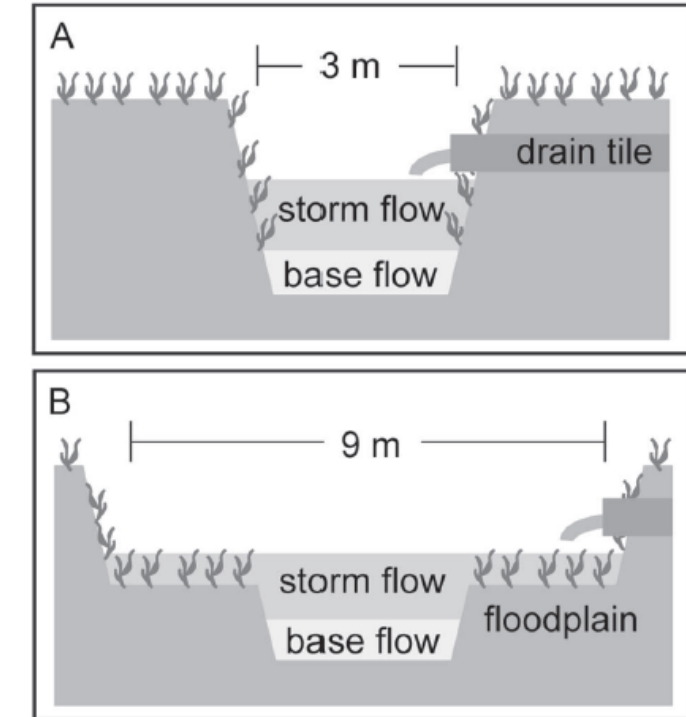


Figure 1. A.—A conventional agricultural ditch. B.—A 2-stage ditch, with floodplains added. Note that the baseflow channel dimensions did not change.

The influence of floodplain restoration on whole-stream metabolism in an agricultural stream: insights from a 5-year continuous data set

Sarah S. Roley^{1,3}, Jennifer L. Tank^{1,4}, Natalie A. Griffiths^{1,5}, Robert O. Hall Jr.^{2,6}, and Robert T. Davis^{1,7}

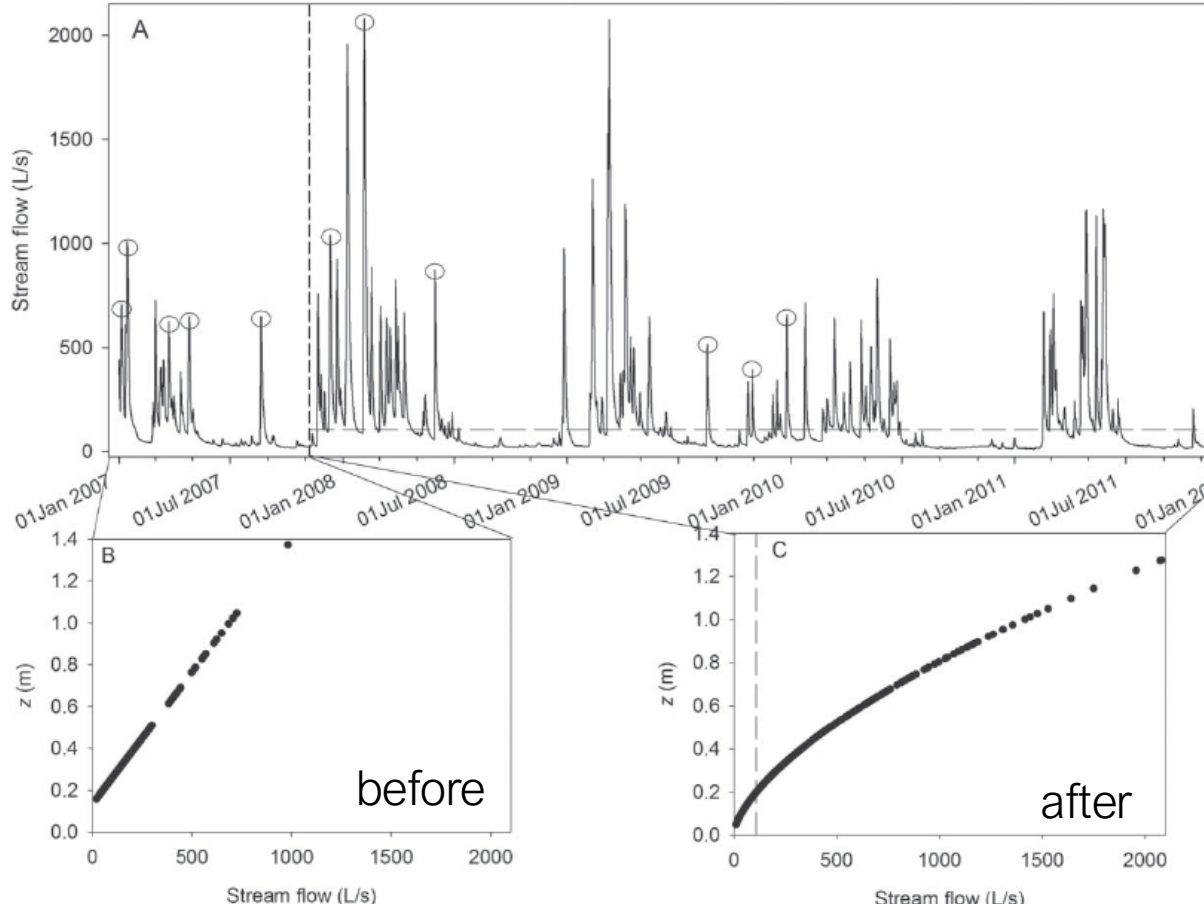


Figure 2. Discharge (Q) in the treatment (TRT) reach (A) and the regression relationship between Q and depth (z) before (B) and after (C) restoration. In panel A, the vertical dashed line represents the 2-stage ditch restoration date and circles indicate the storms analyzed for resistance and resilience. The horizontal line in panel A and the vertical line in panel C represent the Q at which water begins to flow onto the floodplains.

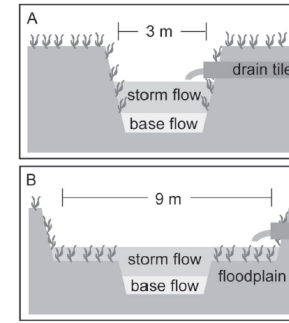


Figure 1. A—A conventional agricultural ditch. B—A 2-stage ditch, with floodplains added. Note that the baseflow channel dimensions did not change.

Restoration changes the relationship between discharge and water depth

The influence of floodplain restoration on whole-stream metabolism in an agricultural stream: insights from a 5-year continuous data set

Sarah S. Roley^{1,3}, Jennifer L. Tank^{1,4}, Natalie A. Griffiths^{1,5}, Robert O. Hall Jr.^{2,6}, and Robert T. Davis^{1,7}

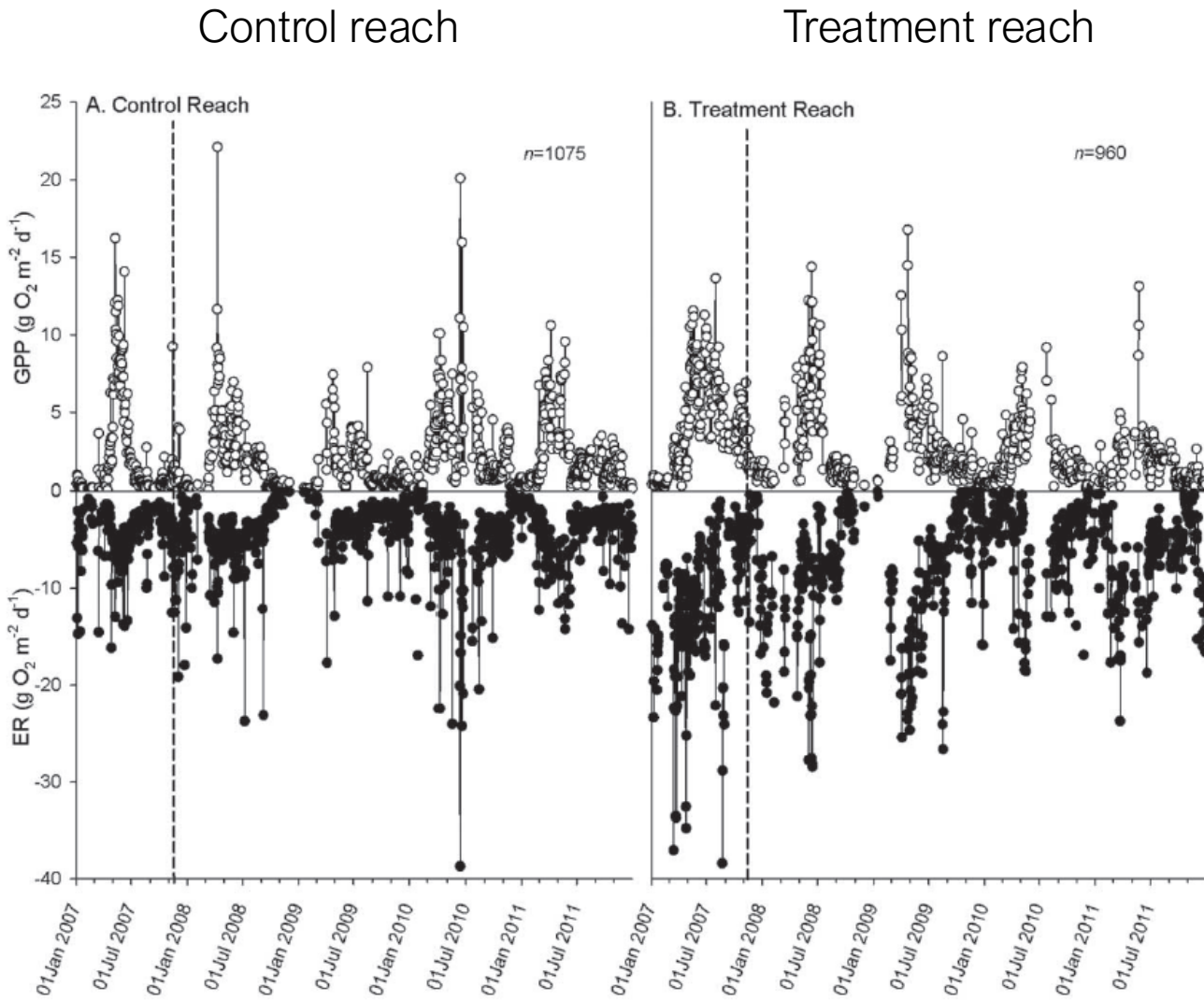


Figure 3. Gross primary production (GPP) and ecosystem respiration (ER) in the control (CTL) (A) and treatment (TRT) (B) reaches. Vertical dashed lines represent the 2-stage ditch restoration date.

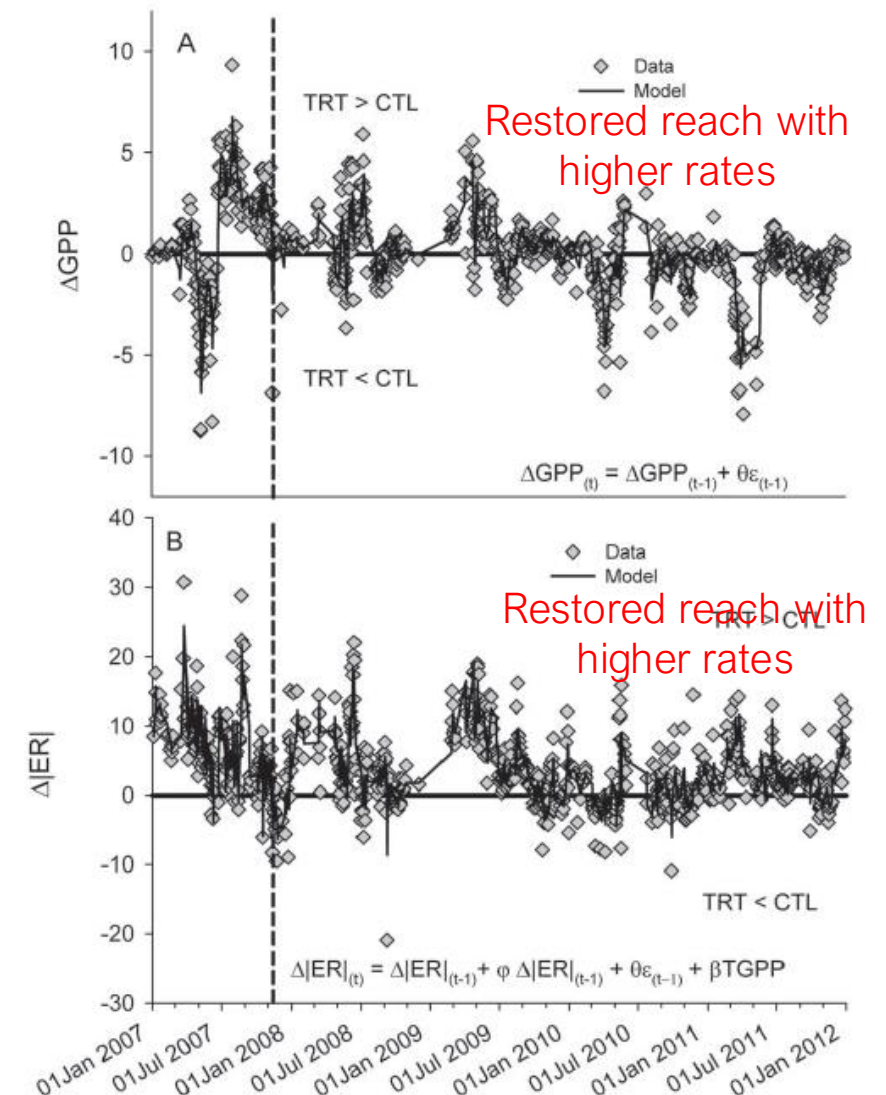
The influence of floodplain restoration on whole-stream metabolism in an agricultural stream: insights from a 5-year continuous data set

Sarah S. Roley^{1,3}, Jennifer L. Tank^{1,4}, Natalie A. Griffiths^{1,5}, Robert O. Hall Jr.^{2,6}, and Robert T. Davis^{1,7}

ΔGPP , ΔER as difference between treatment (restored) and control (non restored)

Restoration of the channel geomorphology increases ecosystem metabolism, both for ER and GPP.

Figure 5. Difference in gross primary production (ΔGPP) (A) and in ecosystem respiration ($\Delta |ER|$) (B) between the treatment (TRT) and control (CTL) reaches with the results of the best-fit auto-regressive integrated moving average (ARIMA) model. Points that fall above 0 are the dates on which the TRT reach had higher rates, and points that fall below 0 are the dates on which the CTL reach had higher rates. The dashed line represents the restoration date. See Table 2 for regression abbreviations.



The metabolic regimes of flowing waters

E. S. Bernhardt ^{1,*} J. B. Heffernan ² N. B. Grimm ³ E. H. Stanley ⁴ J. W. Harvey ⁵,
M. Arroita, ^{6,7} A. P. Appling, ⁸ M. J. Cohen, ⁹ W. H. McDowell ¹⁰ R. O. Hall, Jr., ^{7,a} J. S. Read, ¹¹
B. J. Roberts, ¹² E. G. Stets, ¹³ C. B. Yackulic ¹⁴

Restoring a stream by constructing a wastewater treatment plant

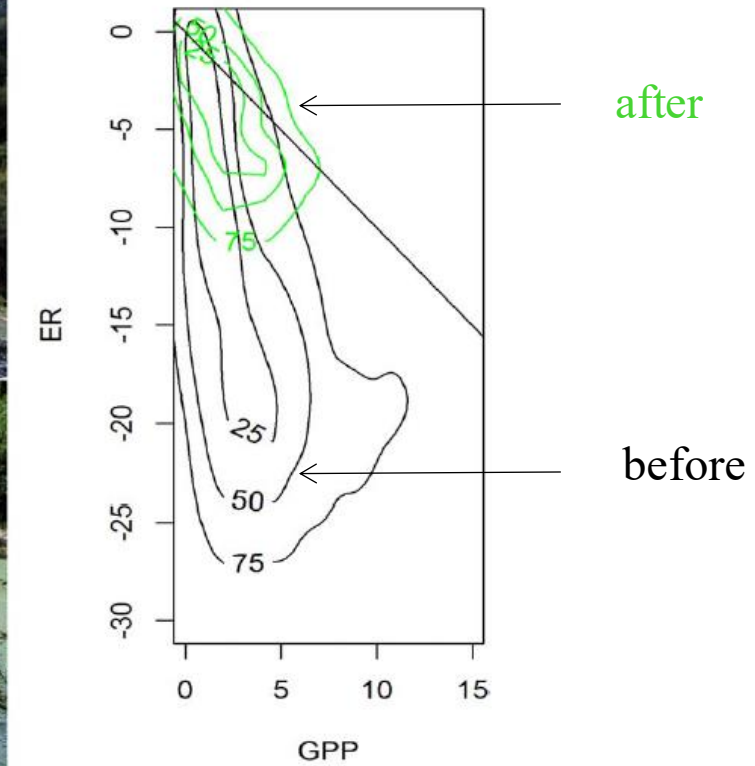
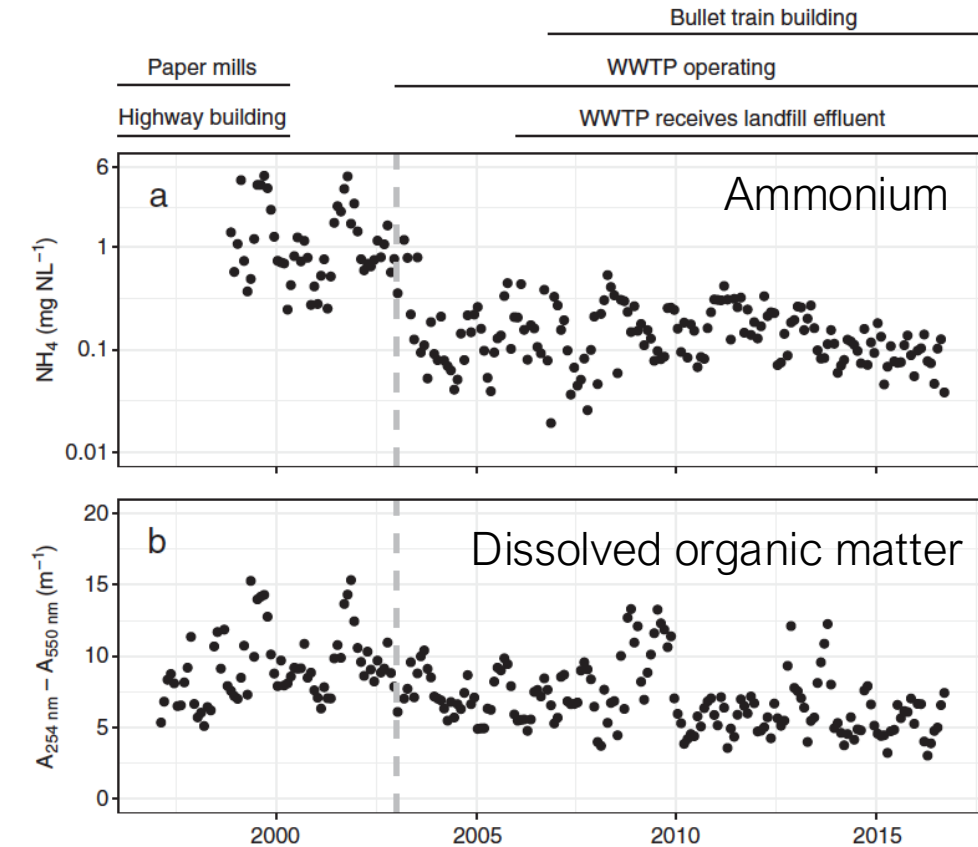


Fig. 8. Two photos of the Oria River and its metabolic fingerprint before (black) and after (green) the construction of a wastewater treatment plant. Photo credits to M. Arroita and A. Elosegi. [Color figure can be viewed at wileyonlinelibrary.com]

Twenty years of daily metabolism show riverine recovery following
sewage abatement

Maite Arroita,^{1,2*} Arturo Elosegi,¹ Robert O. Hall Jr.²



WWTP:

- Immediate effect on ammonium concentration
- Gradual effect on DOM concentration

Fig. 1. Monthly means of ammonium (NH_4) concentration (a) and DOM absorbance (b; $A_{254\text{nm}} - A_{550\text{nm}}$; proxy for DOM concentration) declined following waste water treatment plant installation (dashed gray line). Note log scale for NH_4 .

Twenty years of daily metabolism show riverine recovery following sewage abatement

Maite Arroita,^{1,2*} Arturo Elosegi,¹ Robert O. Hall Jr.²

- GPP summer peaks decreased
- ER decreased over the entire year
- Less heterotrophic ecosystem
- Gas exchange rate increased (absence of algal mats and increasing turbulence)
- Improved aeration
- Higher fish biodiversity

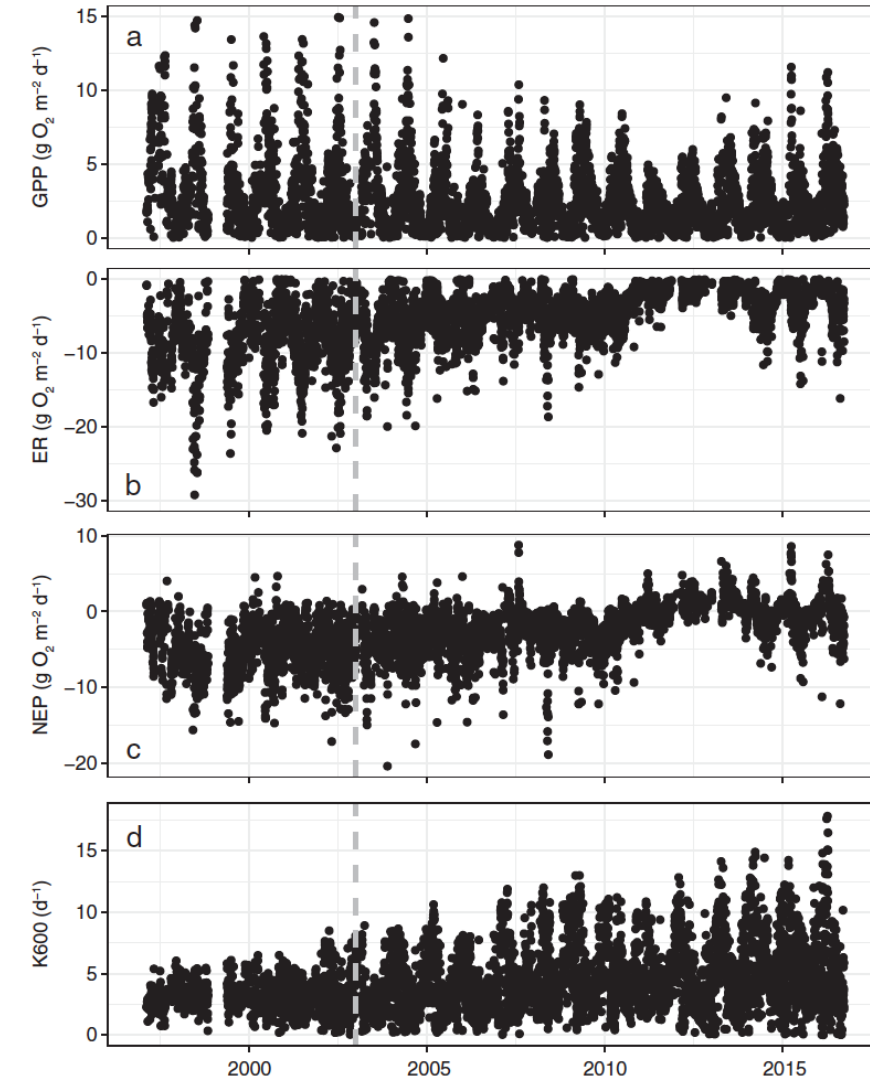


Fig. 2. Following waste water treatment plant installation (dashed gray line) GPP (a) and ER (b) gradually decreased, NEP shifted from highly heterotrophic to a balance between GPP and ER (c), and gas exchange rate coefficient (K600) gradually increased (d).

Areal CO₂ evasion flux decreases downstream

(Why is it so high upstream?)

$$F_{CO2} = k_{CO2} \times \Delta_{CO2}$$

k_{CO2} is the gas exchange velocity for CO₂ (including its diffusivity and solubility)

Δ_{CO2} is the difference in CO₂ concentration between water and CO₂ equilibrium, which is the atmospheric-equilibrium concentration of CO₂.

Distinct air-water gas exchange regimes in low- and high-energy streams

Amber J. Ulseth^{1,4*}, Robert O. Hall Jr², Marta Boix Canadell¹, Hilary L. Madinger^{3,5}, Amin Niayifar¹ and Tom J. Battin¹

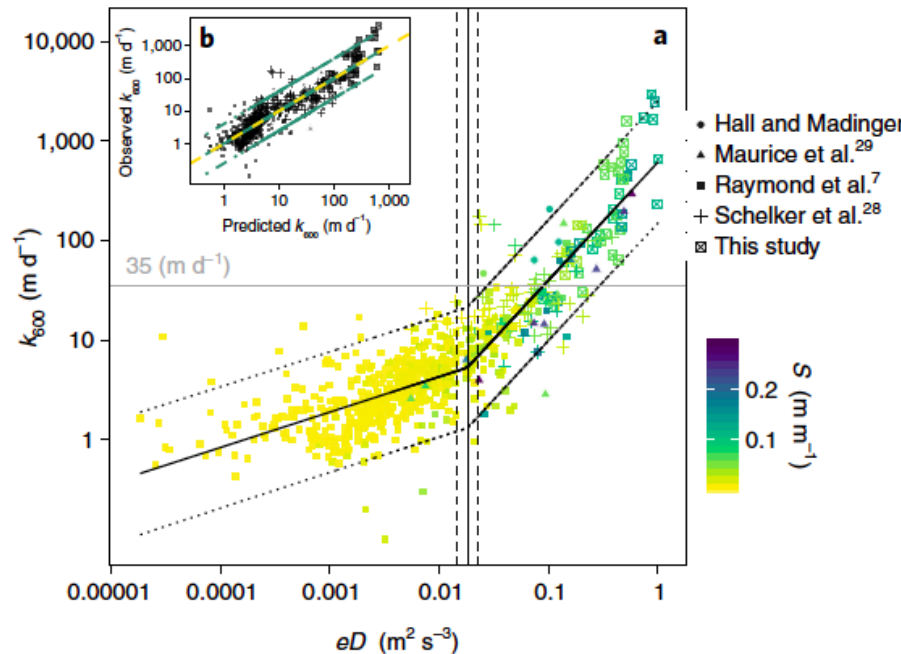


Fig. 2 | k_{600} scaled against eD . **a**, Model fit (black line, with 95%CI shown by dashed lines) estimated using piecewise linear regression analysis ($R^2=0.78$), where $\ln[k_{600}] = 3.10 + 0.35$ (95%CI: 0.31, 0.41) $\times \ln[eD]$ for $eD < 0.02$ (vertical line, dashed vertical lines are 95%CI (0.016, 0.026)) and $\ln[k_{600}] = 6.43 + 1.18$ (95%CI: 1.10, 1.30) $\times \ln[eD]$ for $eD > 0.02$. The grey line theoretically equates to the maximum gas exchange due to diffusivity alone. **b**, The inset shows observed versus predicted k_{600} . The solid green line is the model fit (95%CI, dashed green lines), which falls along the 1:1 line (dashed yellow line).

Areal CO_2 evasion flux decreases downstream
(Why is it so high upstream?)

- Headwater streams often drain terrain with elevated slope.
- This implies higher flow velocity and higher bed roughness (see Hjulstroem).
- Roughness and velocity affect energy dissipation (eD ; velocity, slope and gravity) at the streambed — increasing turbulence at the streambed propagated to the water surface.
- Turbulence advects gases through the water surface.
- High turbulence entrains air bubbles (white waters) into the water — increasing surface area for gas exchange.

Areal CO_2 evasion flux decreases downstream (Why is it so high upstream?)

Distinct air-water gas exchange regimes in low- and high-energy streams

Amber J. Ulseth^{1,4*}, Robert O. Hall Jr², Marta Boix Canadell¹, Hilary L. Madinger^{3,5}, Amin Niayifar¹ and Tom J. Battin¹

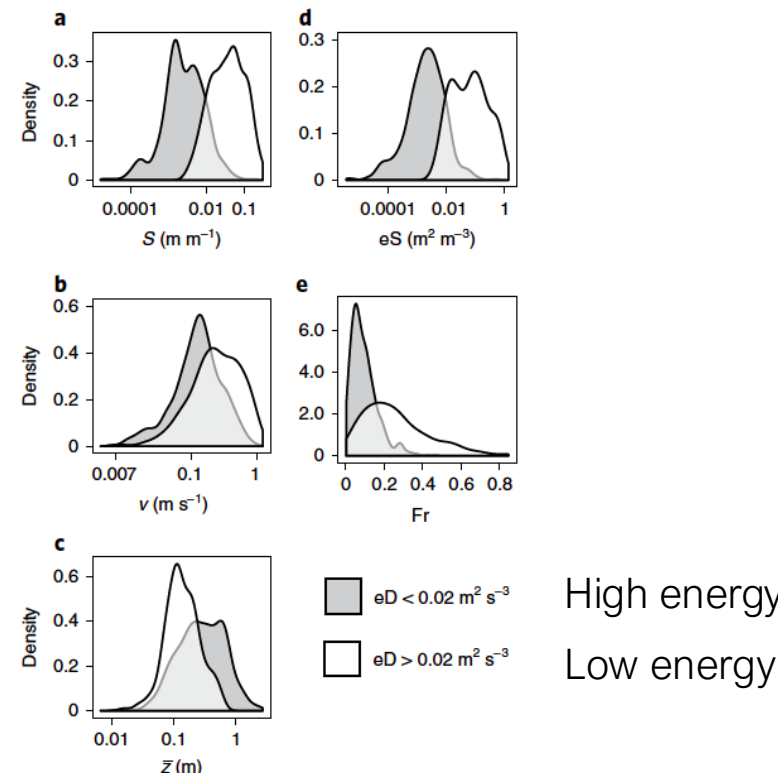


Fig. 3 | Density distributions of stream characteristics for low- versus high-energy streams. **a–e**, Streams with eD higher than the breakpoint ($eD > 0.02 \text{ m}^2 \text{ s}^{-3}$) in Fig. 2 had steeper S (**a**), higher eS (**d**) and higher Froude number (**e**) than those below the breakpoint, as illustrated by the density distributions, while there was greater overlap above and below the breakpoint for stream v (**b**) and z (**c**).

- Hydraulics and hydraulic geometry different in high- than low-energy streams.
- Hydraulics related to roughness affects gas exchange velocity
- Changes predictably along the fluvial continuum

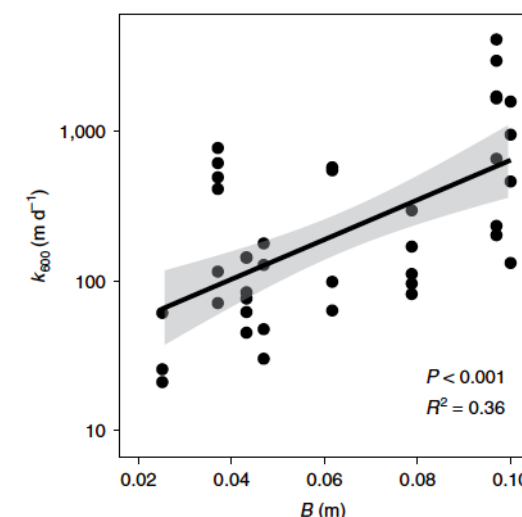


Fig. 4 | Gas exchange increased with streambed roughness. k_{600} increased with median streambed roughness (B) across eight of the Swiss alpine stream reaches. The black line is the fit from semi-natural log linear regression, $\ln[k_{600}] = 3.41 + 30.52 \times B$, and the grey band represents 95%CI of the predicted k_{600} .

Unexpected large evasion fluxes of carbon dioxide from turbulent streams draining the world's mountains

Åsa Horgby¹, Pier Luigi Segatto¹, Enrico Bertuzzo², Ronny Lauerwald³, Bernhard Lehner¹,
Amber J. Ulseth⁵, Torsten W. Vennemann⁶ & Tom J. Battin^{1*}

Mountain streams worldwide are major sources of CO₂ to the atmosphere.

Unexpected because of their relatively low surface area and catchments that are often devoid of terrestrial vegetation and soils.

Steep slopes, high gas transfer

Well connected to groundwater – CO₂ from soil respiration and rock weathering

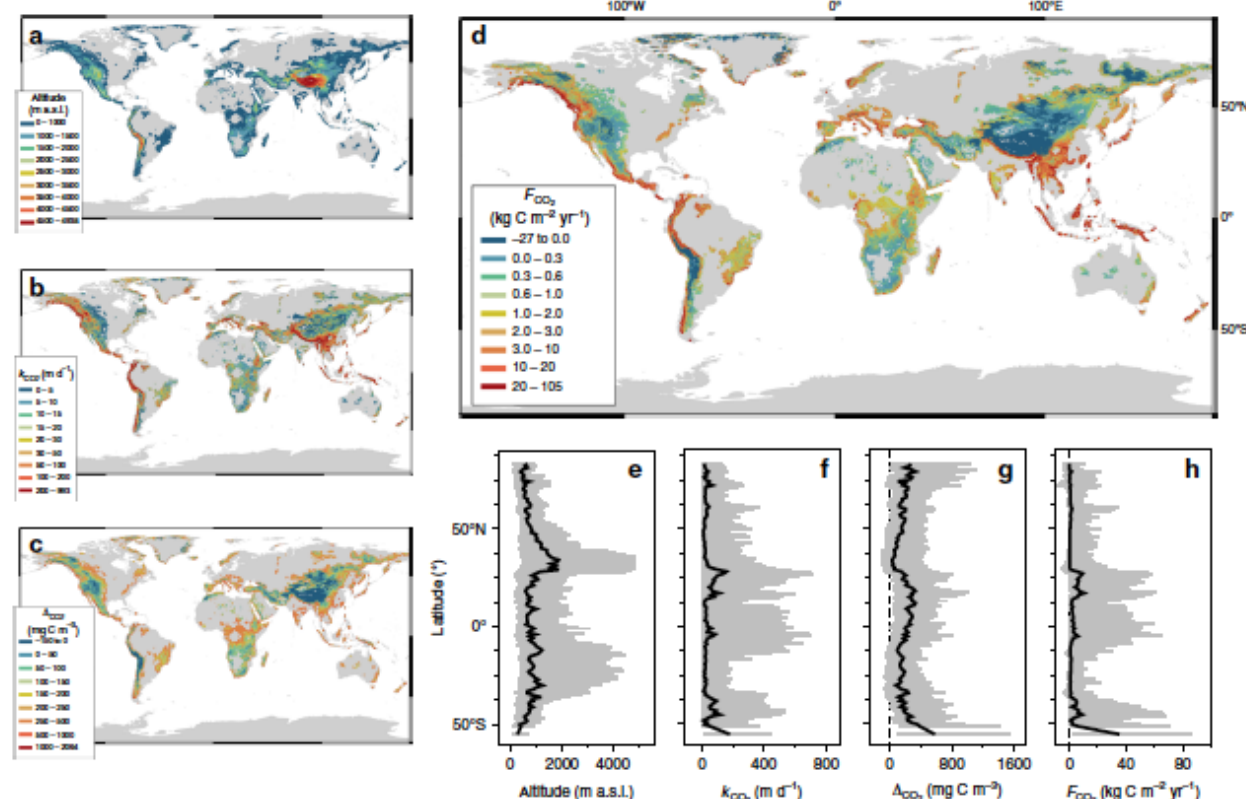


Fig. 3 Global distributions of CO₂ in mountain streams. **a** Altitude of mountain streams, where mountains as defined according to ref. ⁷. **b-d** Global distribution of predicted CO₂ exchange velocities (k_{CO_2}), CO₂ gradients between the streamwater and the atmosphere (Δ_{CO_2}) and the areal CO₂ fluxes (F_{CO_2}), respectively. **e-h** Latitudinal transects of these same parameters at 1-degree resolution (shown are median values in black and 5 and 95% confidence intervals in gray).

LETTER

Gas transfer velocity (k_{600}) increases with discharge in steep streams but not in low-slope streams

Kelly S. Aho ¹*, Kaelin M. Cawley ², Robert O. Hall Jr. ³, Robert T. Hensley ¹, ², Walter K. Dodds ¹, ⁴
Nicolas Harrison, ² Keli J. Goodman ²

339 gas tracer experiments to measure gas transfer velocity (k_{600})

Relate k_{600} to discharge and energy dissipation (eD)

How does k_{600} react to varying discharge in high- versus low-slope streams?

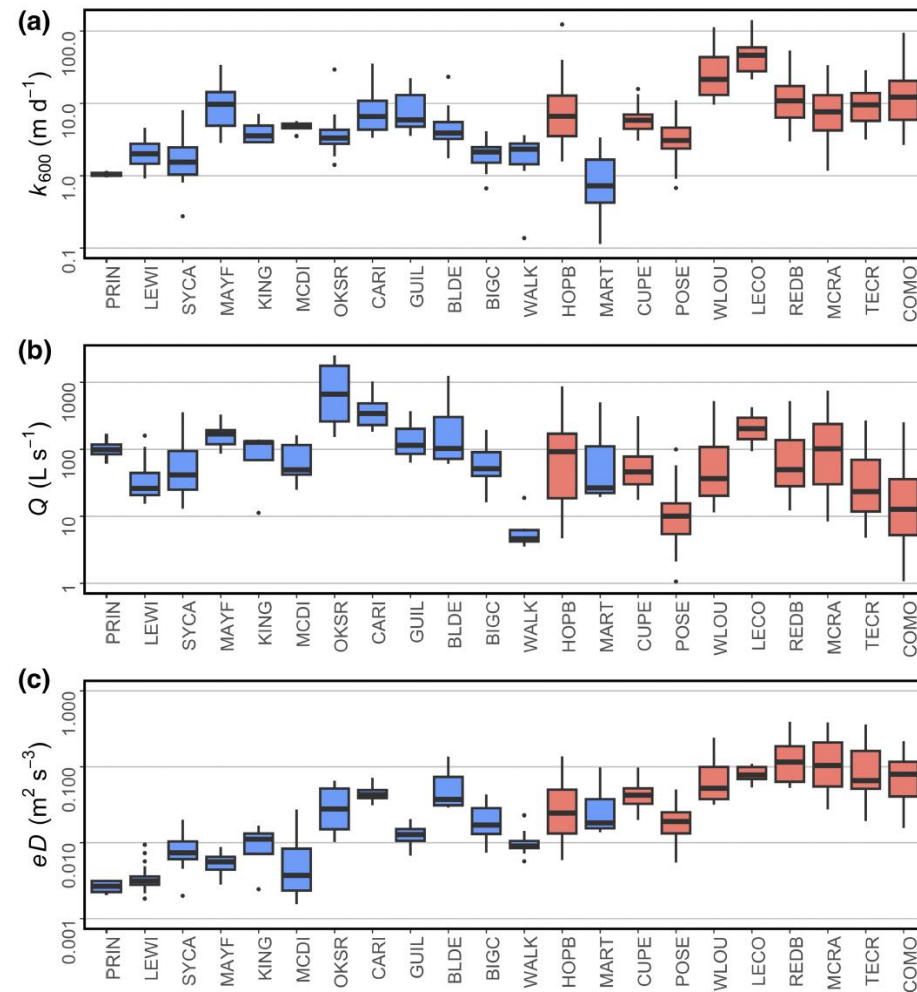


Fig. 1. **(a)** Gas transfer velocity (k_{600}), **(b)** discharge (Q), and **(c)** energy dissipation (eD) for each tracer-gas experiment by site. Sites are arranged in order of increasing slope (e.g., lowest gradient: PRIN; highest gradient: COMO). Boxes represent the median and interquartile range (IQR), whiskers mark the lesser of $1.5 \times \text{IQR}$ or minimum/maximum, and points denote outliers more extreme than $1.5 \times \text{IQR}$. Color of the text indicate if k_{600} for the site had a low (blue) or high (red) Q dependency.

LETTER

Gas transfer velocity (k_{600}) increases with discharge in steep streams but not in low-slope streams

Kelly S. Aho ^{1,*}, Kaelin M. Cawley, ², Robert O. Hall Jr., ³, Robert T. Hensley ^{1,2}, Walter K. Dodds ^{1,4},
Nicolas Harrison, ² and Keli J. Goodman²

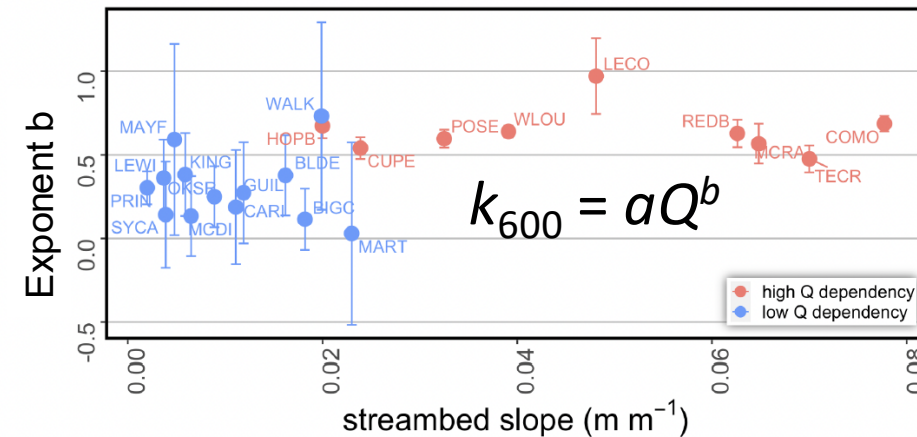


Fig. 3. Estimates of the exponent b of the power law relationship $k_{600} = aQ^b$ for each of the 22 NEON sites arranged in order of increasing slope. The error bars represent the standard deviation of the estimate. Colors indicate whether k_{600} for the site had a low (blue) or high (red) Q dependency.

- Gas exchange velocity in high-slope streams reacts more to increases in discharge than in low-slope streams
- Effect of energy dissipation (velocity, slope and gravity) more pronounced in high-slope streams
- Results from turbulence as induced by roughness and velocity

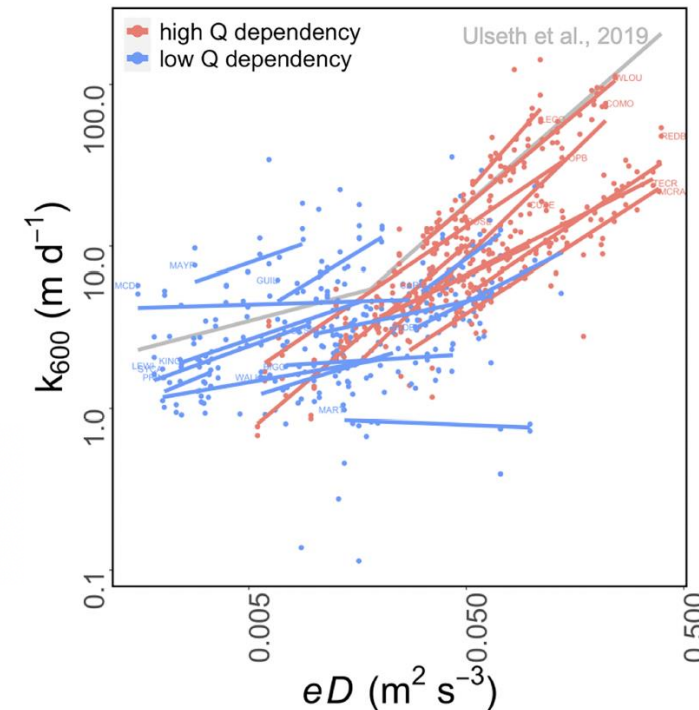


Fig. 4. Relationship between eD and k_{600} by site. The input data are shown as points, and the fitted values from the mixed-effect model are shown as lines. Colors indicate if the site had a low (blue) or high (red) Q dependency for k_{600} . For context, the gray line shows the two-stage model presented in Ulseth et al. (2019).

Sources of and processes controlling CO₂ emissions change with the size of streams and rivers

E. R. Hotchkiss^{1*†}, R. O. Hall Jr², R. A. Sponseller¹, D. Butman³, J. Klaminder¹, H. Laudon⁴, M. Rosvall⁵ and J. Karlsson¹

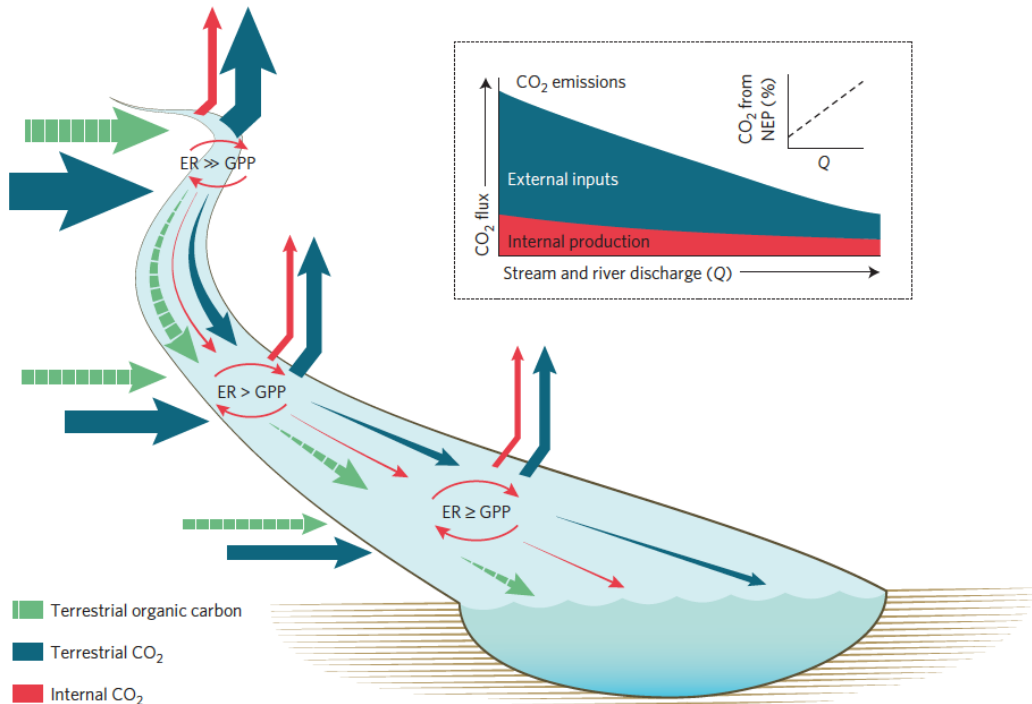
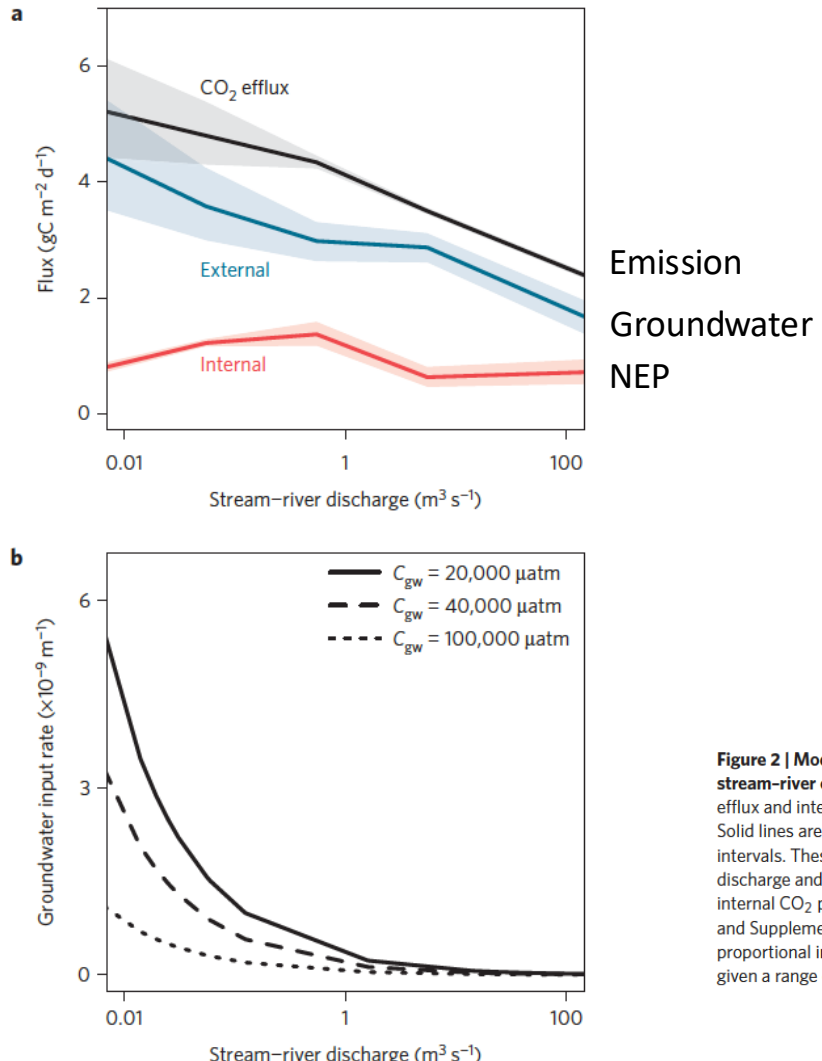


Figure 3 | Sources and magnitude of net CO₂ emissions along a theoretical stream-river continuum. Terrestrially derived CO₂ and organic carbon inputs per unit aquatic area decline downstream, decreasing net CO₂ emission rates in rivers compared to streams. Rapid loss of CO₂ results in a downstream shift in the source contributions to CO₂ emissions, from dominance of external CO₂ in streams to a more balanced supply of internal and external sources in rivers. Thus, aquatic mineralization of terrestrial OC (CO₂ from NEP) should contribute to a higher proportion of annual net CO₂ emissions in large rivers relative to small streams.

- Both sources and magnitude of the CO₂ evasion change downstream
- Allochthonous organic carbon and CO₂ prevail in headwaters
- Allochthonous sources decline downstream because connectivity with the catchment decreases
- Ecosystems (internal) production of CO₂ decreases as well because the ratio of sediment to water decreases (see streambed as bioreactor)

Sources of and processes controlling CO₂ emissions change with the size of streams and rivers

E. R. Hotchkiss^{1*}†, R. O. Hall Jr², R. A. Sponseller¹, D. Butman³, J. Klaminder¹, H. Laudon⁴, M. Rosvall⁵ and J. Karlsson¹



Areal CO₂ evasion flux decreases downstream
(Why is it so high upstream?)

CO₂ contributions from the groundwater decrease downstream

Figure 2 | Modelled CO₂ fluxes and groundwater input rates along a stream-river continuum. **a**, Binned discharge-specific estimates for CO₂ efflux and internal production and, by subtraction, external CO₂ inputs. Solid lines are median fluxes; shaded regions represent 25–75% credible intervals. These fluxes were used to model the range of groundwater discharge and input rates needed to sustain a steady state balance between internal CO₂ production, external CO₂ inputs and CO₂ efflux (see Methods and Supplementary Section 2). **b**, Modelled stream-river groundwater proportional input rates (k_{gw}) needed to support estimated CO₂ fluxes (**a**) given a range of potential groundwater CO₂ concentrations (C_{gw}).

CO₂ evasion along streams driven by groundwater inputs and geomorphic controls

Clément Duvert¹*, David E. Butman², Anne Marx³, Olivier Ribolzi⁴ and Lindsay B. Hutley¹

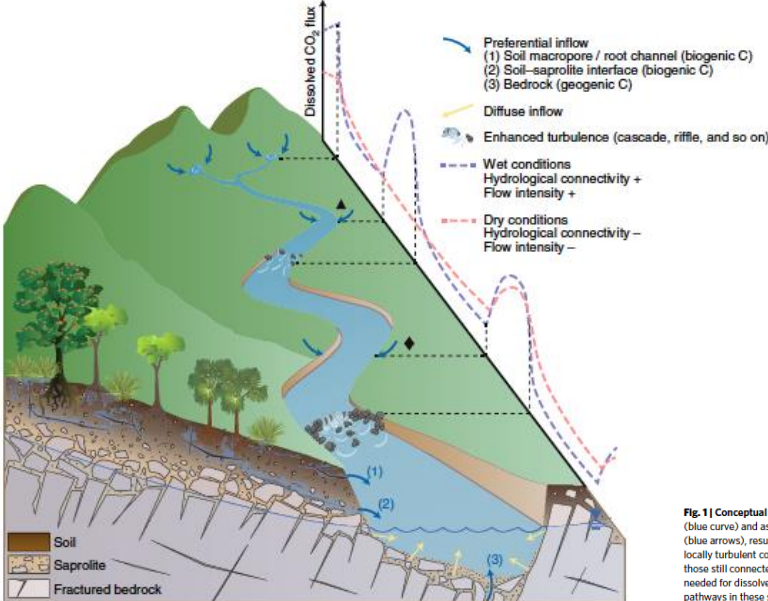


Fig. 1 | Conceptual diagram of the subsurface and stream heterogeneities contributing to CO₂ variations in headwater streams. Under wet cond (blue curve) and assuming high terrestrial primary productivity, subsurface flowpaths connect soil CO₂ sources to streams via high-conductivity p (blue arrows), resulting in large CO₂ pulses along streams. Rapid evasion is favoured by in-stream geomorphic controls such as cascades or riffles locally turbulent conditions. Under drier conditions (pink curve), not all flowpaths are connected to streams (for example, inflow area marked ▲), those still connected may carry lower rates of water and CO₂ (for example, inflow area marked ●). Lower turbulence results in longer distances be needed for dissolved CO₂ to evade streams. Diffuse, low-magnitude groundwater inflow (yellow arrows) may be less significant than preferential i pathways in these systems.

- Channel and valley geomorphology drives groundwater inputs
- Groundwater inputs are hotspots of CO₂ outgassing
- Particularly pronounced in headwater streams that are tightly connected to groundwater
- Rapid outgassing depending on channel geomorphology and turbulence

CO₂ contributions from the groundwater decrease downstream (Why are they so high upstream?)

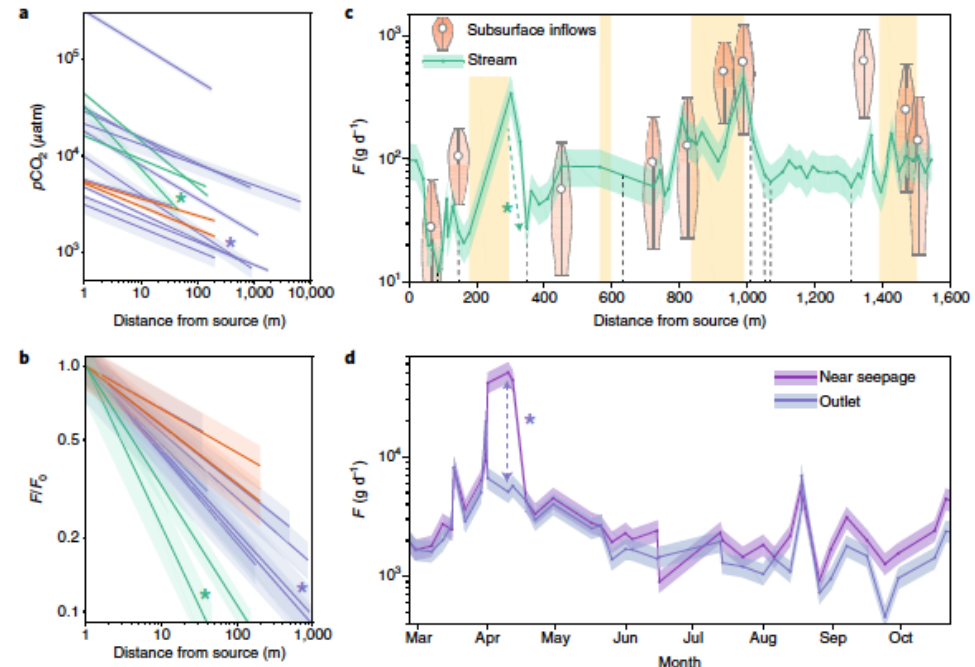


Fig. 2 | Illustration of CO₂ evasion within short distance of subsurface inflows. **a**, Decrease in the partial pressure of CO₂ (p_{CO_2}) values from emerging groundwater to streams. Green, blue and brown represent tropical, temperate and boreal streams, respectively. The shaded areas around each line represent measurement uncertainties as described in the Supplementary Information. The two lines marked with green and purple asterisks in **a** and **b** correspond to data collected as part of this study in Houay Pano (Laos) and Uhlírská (Czech Republic), respectively. All other lines are taken from the literature (see Supplementary References). **b**, Decrease in flow-weighted CO₂ flux (F) from emerging groundwater to streams. Values have been normalized to the subsurface (source) CO₂ flux F_0 to facilitate inter-site comparison. **c**, Longitudinal profile of dissolved CO₂ flux along a steep tropical headwater stream in northern Laos (Houay Pano, 0.64 km²). The green curve represents the in-stream CO₂ flux with its 10th–90th percentile uncertainty range (see Supplementary Information). Yellow shaded areas represent locations of flatter reaches that support riparian vegetation with diffuse inflow of groundwater. Violin plots represent the measured CO₂ inputs delivered by preferential subsurface inflows with their 10th–90th percentile range. Black vertical dotted lines correspond to locations with higher turbulence, such as minor falls. The green asterisk refers to the data points used in **a** and **b**. **d**, Temporal variations in dissolved CO₂ flux along a temperate headwater stream in the Czech Republic (Uhlírská, 1.78 km²). Data were collected in shallow groundwater and at two stream locations, immediately downstream of a subsurface seepage area and at the outlet of the catchment, 900 m downstream of the seepage. The shaded areas around each curve represent their 10th–90th percentile uncertainty ranges. The purple asterisk corresponds to the data points used in **a** and **b**.

Toward Modeling Continental-Scale Inland Water Carbon Dioxide Emissions

Brian Saccardi¹ , Craig B. Brinkerhoff² , Colin J. Gleason² , and Matthew J. Winnick¹ 

Brian Saccardi and Craig B. Brinkerhoff contributed equally to this work.

Groundwater CO₂ inputs matter, but is it all?

CO₂ transport model for the continental USA simulating carbon transport and transformation in more than 22 million hydraulically connected rivers, lakes, and reservoirs

Stream corridor (comprising stream benthic zones, the hyporheic zone, and near-stream riparian zones and floodplains) CO₂ production dominates over groundwater inputs at the continental scale

Water column respiration more important downstream

Depending on stream order!

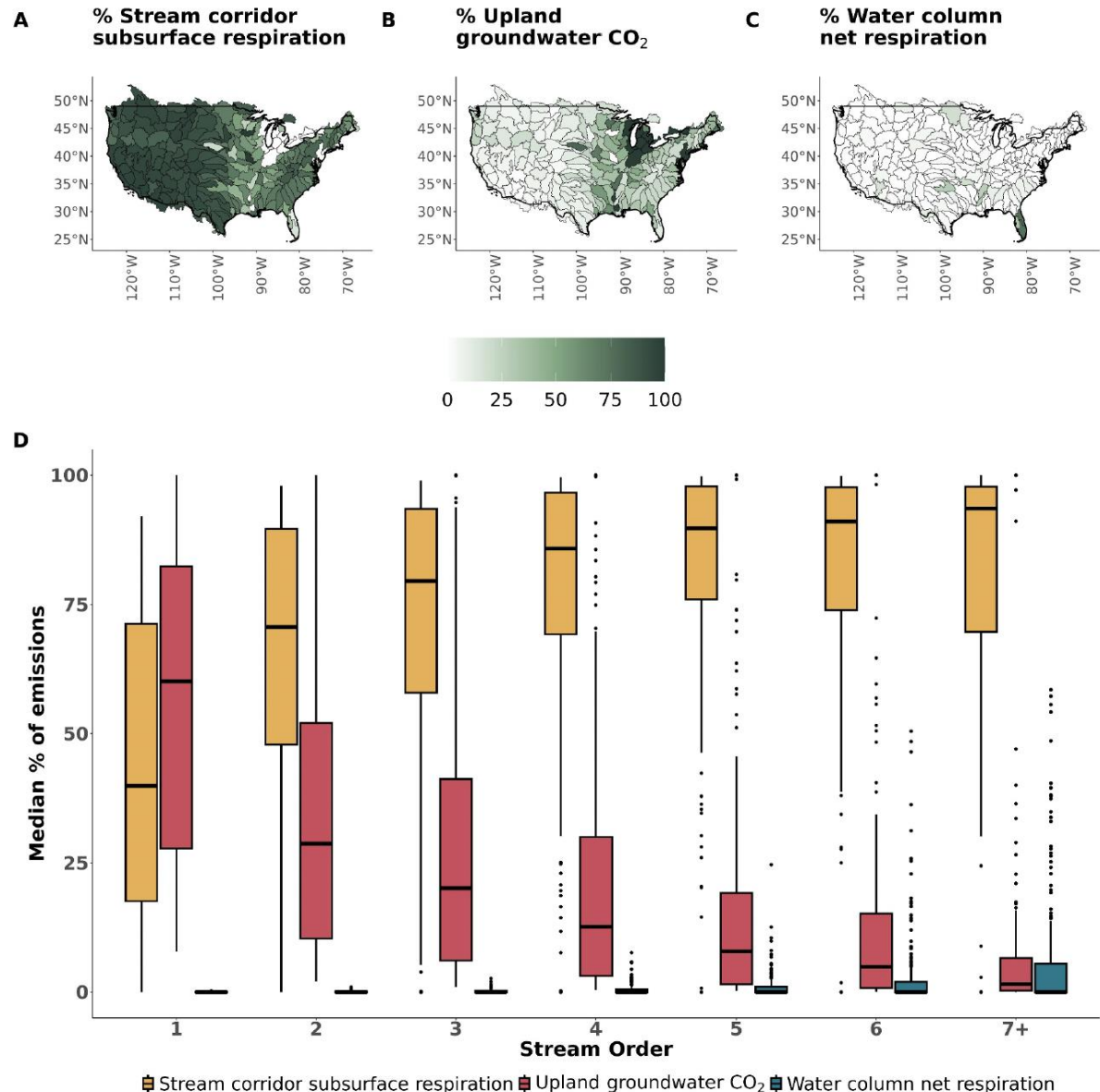


Figure 3. Sources of inland water CO₂ emissions. a–c: Percent of CO₂ lost from a basin that is attributed to stream corridor subsurface respiration (a), upland groundwater CO₂ (b), and net water-column respiration (c). (d) Percent of CO₂ emissions attributed to the same mechanisms as a–c by stream order; boxplots are composed of the median percent value per basin per stream order. See Section 2 for these calculations at the basin-scale (a–c) and the reach-scale (d). Note we lump high stream orders (seven and above) due to the small number of basins with this many stream orders and to represent network main stems as a single boxplot. Figure S9 in Supporting Information S1 separates d by eastern and western CONUS basins.

Temporal variation of CO₂ outgassing

Seasonal

AGU PUBLICATIONS



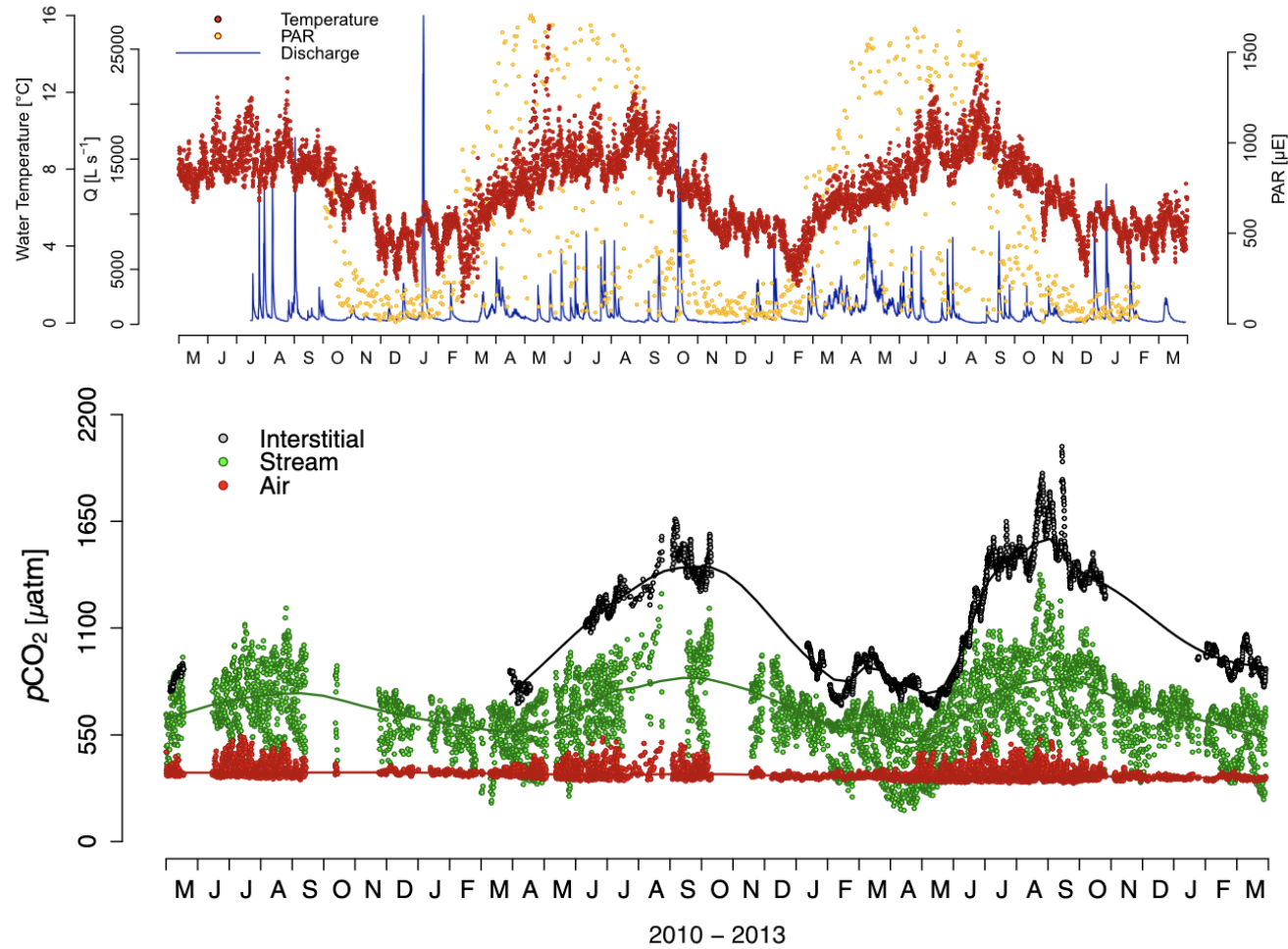
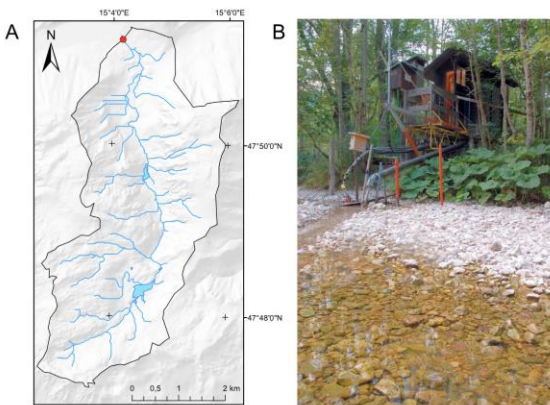
Journal of Geophysical Research: Biogeosciences

RESEARCH ARTICLE
10.1002/2013JG002552

Key Points:
• High temporal dynamics of pCO₂ in streams

Scales and drivers of temporal pCO₂ dynamics
in an Alpine stream

Hannes Peter¹, Gabriel A. Singer^{2,3,4}, Christian Preller², Peter Chifford⁵, Gertraud Stenicka²,
and Tom J. Battin^{2,3}



- Distinct seasonal patterns of streamwater pCO₂
- More pronounced in the hyporheic than surface water
- Few instances of CO₂ undersaturation — in spring, because of positive NEP

Temporal variation of CO₂ outgass

Diel and event-driven

AGU PUBLICATIONS



Journal of Geophysical Research: Biogeosciences

RESEARCH ARTICLE
10.1002/2013JG002552

Key Points:
• High temporal dynamics of pCO₂ in streams

Scales and drivers of temporal pCO₂ dynamics
in an Alpine stream

Hannes Peter¹, Gabriel A. Singer^{2,3,4}, Christian Preller², Peter Chifford⁵, Gertraud Steniczka²,
and Tom J. Battin^{2,3}

Sub-seasonal variation

- Pronounced day-night cycles of streamwater pCO₂ in summer, less in winter
- Night peaks indicate ecosystem respiration dominating over production
- Post-storm diel pattern indicates recovery and active biomass buildup

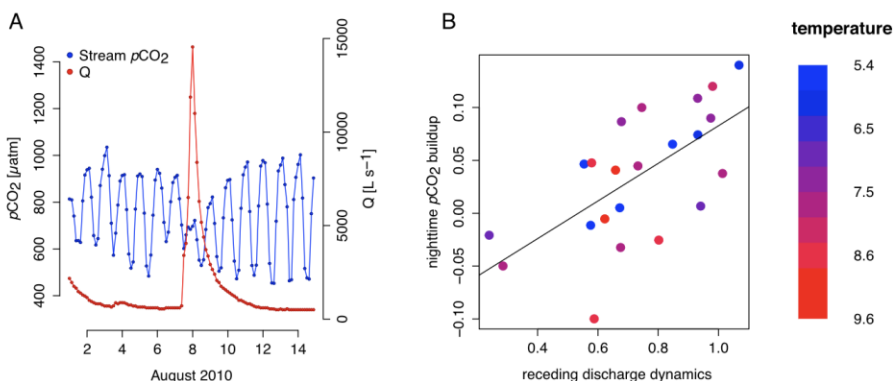
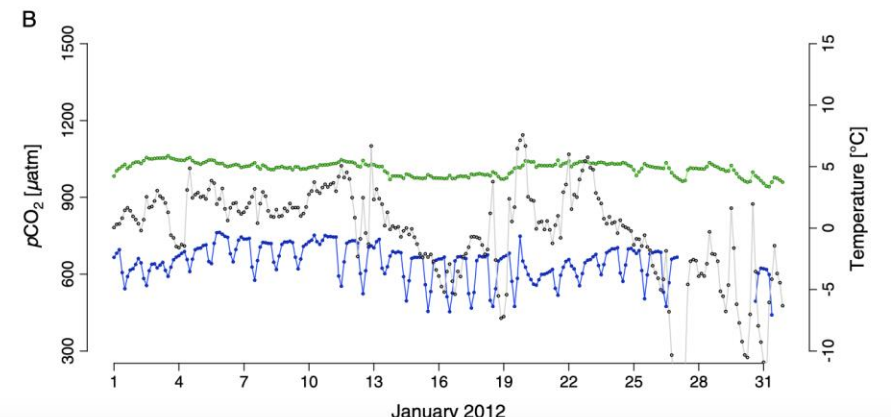
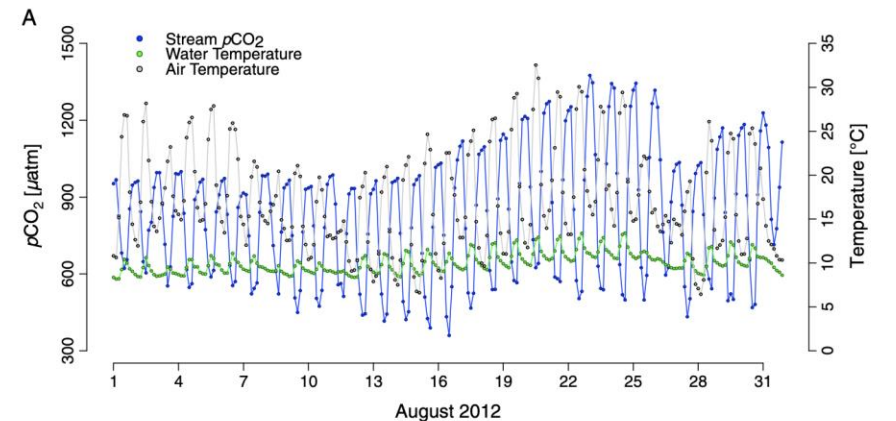


Figure 5. Event-driven pCO₂ dynamics in the stream water in Oberer Seebach. A bed-moving storm event ($Q > 3400 \text{ L s}^{-1}$) causes the collapse of the diurnal stream water pCO₂ patterns (a). The relationship between the recovery dynamics of nighttime pCO₂ maxima and the recession dynamics of discharge is also shown (b). Plotted are the exponents of power models fitted to the discharge and stream water pCO₂ maxima over 6 days after peak discharge.

Temporal variation of CO₂ outgassing

Diel



Global carbon dioxide efflux from rivers enhanced by high nocturnal emissions

Lluís Gómez-Gener^{1,2,4}, Gerard Rocher-Ros^{2,24}, Tom Battin¹, Matthew J. Cohen³, Hugo J. Dalmagro^{2,4}, Kerry J. Dinsmore⁵, Travis W. Drake⁶, Clément Duvert⁷, Alex Enrich-Prast^{8,9}, Asa Horgby¹⁰, Mark S. Johnson^{10,11}, Lily Kirk¹², Fausto Machado-Silva⁹, Nicholas S. Marzolf¹³, Mollie J. McDowell^{10,11}, William H. McDowell¹⁴, Heli Miettinen¹⁵, Anne K. Ojala¹⁶, Hannes Peter¹, Jukka Pumpanen¹⁷, Lishan Ran¹⁸, Diego A. Riveros-Iregui¹⁹, Isaac R. Santos²⁰, Johan Six⁴, Emily H. Stanley²¹, Marcus B. Wallin²², Shane A. White²³ and Ryan A. Sponseller²

- Overall higher nocturnal CO₂ emissions – independent of the biome
- Highest diel variation in open-canopy streams during summer (light, primary production)
- Important when scaling CO₂ emissions up to assess the role of streams and rivers for the global carbon cycle

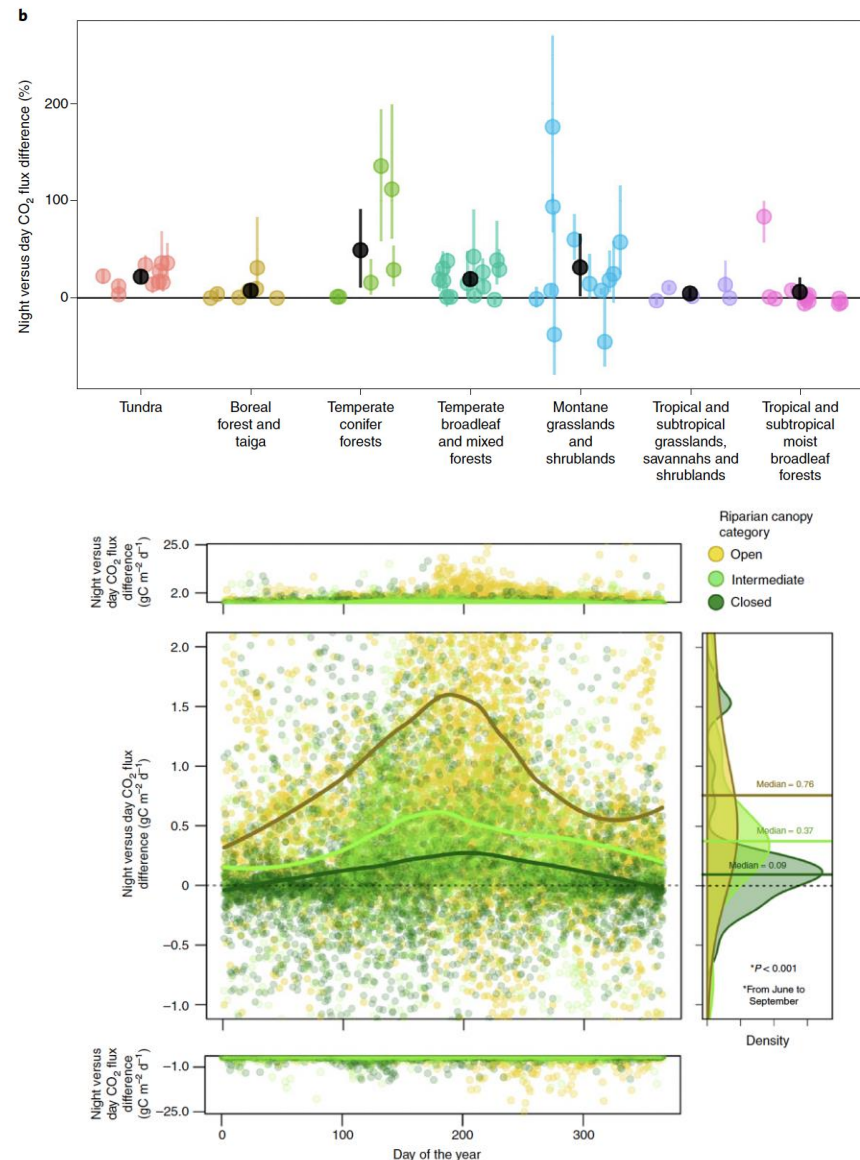
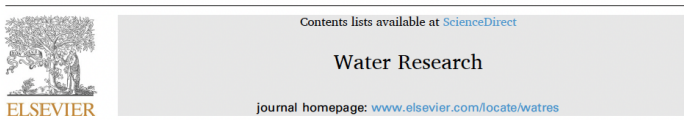


Fig. 3 | Seasonal pattern of diel changes in CO₂ emission fluxes from streams. Seasonal variation in the night versus day difference of CO₂ emission fluxes ($\text{gC m}^{-2} \text{d}^{-1}$) grouped by riparian canopy-cover category (open, yellow; intermediate, light green; closed; dark green; 33, 16 and 17 sites and 5,780, 3,814 and 5,130 daily observations, respectively; see Methods and Supplementary Table 2). The coloured solid lines are locally weighted (loess) regression model fits for a visual interpretation. Panels at the top and bottom show extreme positive and negative values, respectively (note change in scaling). Density plots show distributions of night versus day differences of CO₂ emission fluxes ($\text{gC m}^{-2} \text{d}^{-1}$) grouped by canopy cover during summer. Differences between canopy levels were evaluated using the non-parametric Kruskal-Wallis test.

Temporal variation of CO₂ outgassing

Drying and diel

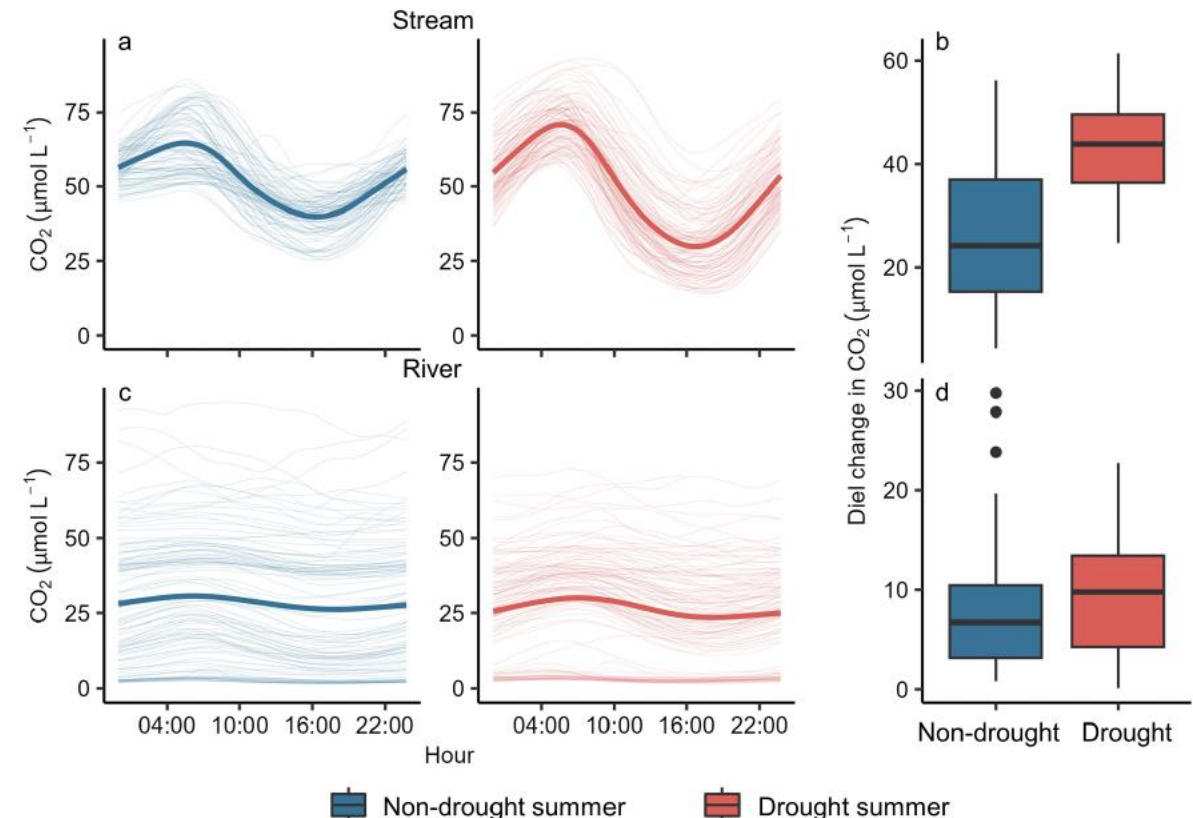
Water Research 271 (2025) 122870



Summer drought enhances diurnal amplitude of CO₂ in two German rivers of different size

Peifang Leng ^{a,b,*}, Michael Rode ^c, Matthias Koschorreck ^b

- Stronger diel variation in CO₂ concentration in small streams compared to larger rivers
- Drought effect on diel variation stronger in streams
- Attributable to decreasing depth, rather than temperature and light availability – probably linked to oxygenation



Greenhouse gas emissions from drying streams and rivers



Emissions from dry inland waters are a blind spot in the global carbon cycle
Rafael Marcé^a, Biel Obrador^a, Lluís Gómez-Gener^a, Núria Catalán^a, Matthias Koschorreck^{a,l},
María Isabel Arce^c, Gabriel Singer^c, Daniel von Schiller^a

- Climate change
- Irrigation
- Water diversion

Greenhouse gas emissions from drying streams and rivers

Received: 28 December 2022 | Revised: 31 July 2023 | Accepted: 18 August 2023
DOI: 10.1111/fwb.14172

REVIEW

Freshwater Biology | WILEY

Greenhouse gas dynamics in river networks fragmented by drying and damming

Teresa Silverthorn¹ | Naiara López-Rojo² | Arnaud Foulquier² | Vincent Chanudet³ | Thibault Datry¹

Drying and rewetting streams and rivers are significant sources of greenhouse gases to the atmosphere

- Elevated temperature
- Anoxic/hypoxic conditions
- Increased residence times
- Organic matter accumulation

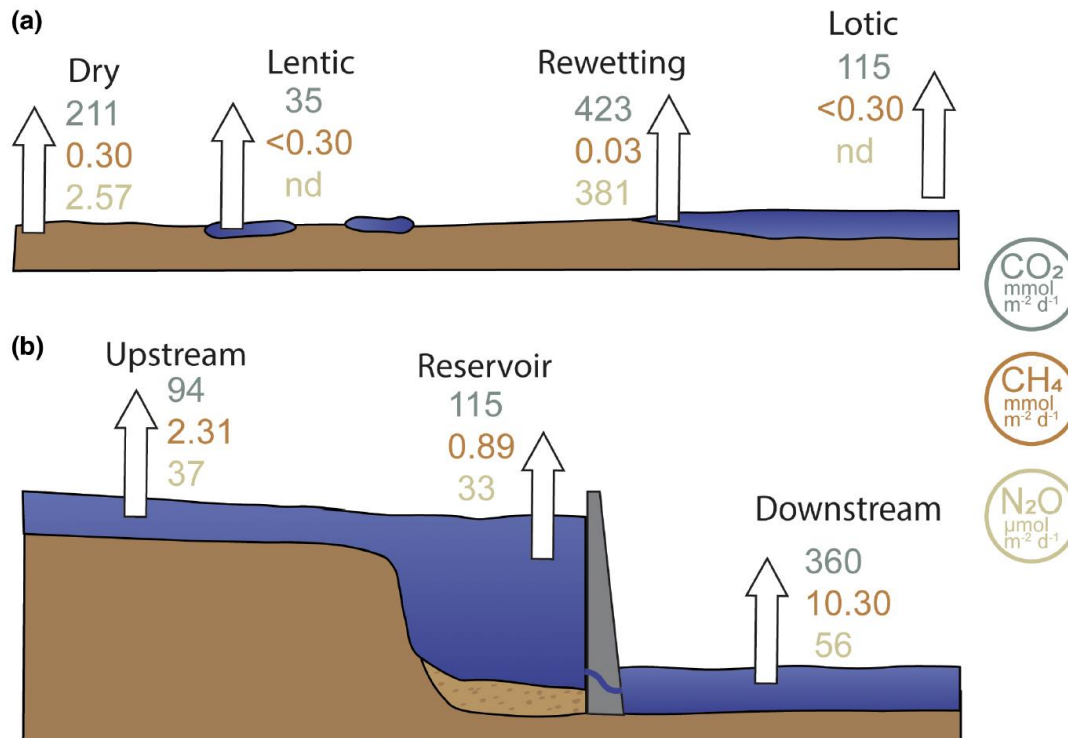


FIGURE 3 Comparison of mean greenhouse gas fluxes from dry sediments (Dry), isolated pools (Lentic), rewetting (Rewetting) and lotic waters (Lotic) in intermittent rivers and ephemeral streams (IRES) (a), as well as reservoirs and their associated (upstream and downstream) rivers (b). Carbon dioxide (CO₂) and methane (CH₄), in blue and orange text, respectively, are reported in units of (mmol m⁻² day⁻¹). Nitrous oxide (N₂O), in yellow text, is reported in units of μmol m⁻² day⁻¹. nd, no available data from our literature search. For the full data from our literature review used to make this figure, see Tables S3–S6.

Greenhouse gas emissions from drying streams and rivers

ARTICLES

<https://doi.org/10.1038/s41561-021-00734-z>

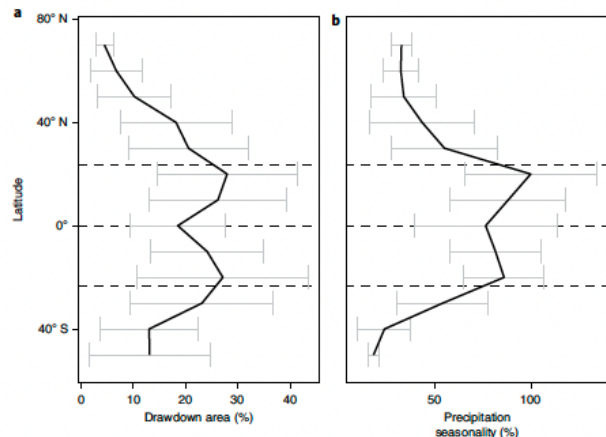
nature
geoscience

Check for updates

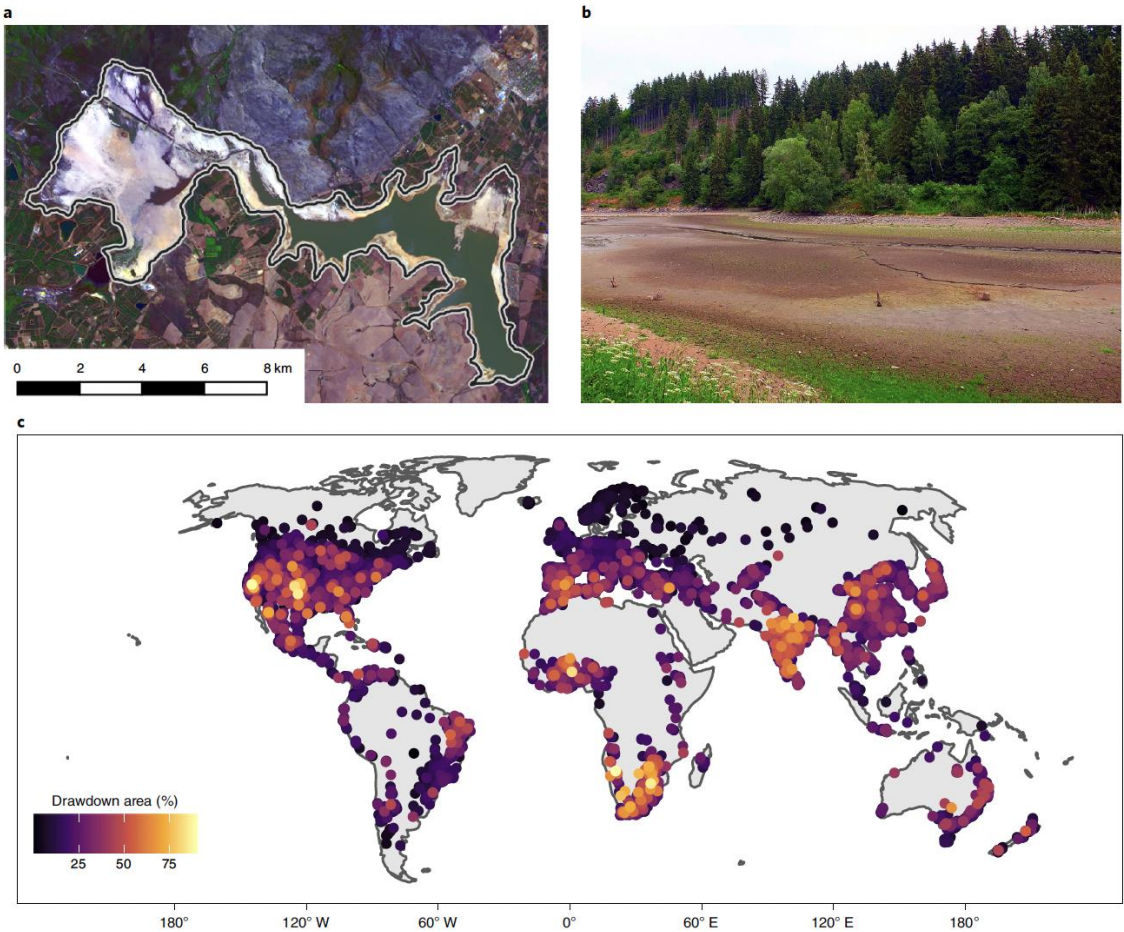
OPEN

Global carbon budget of reservoirs is overturned by the quantification of drawdown areas

Philipp S. Keller¹✉, Rafael Marcé^{2,3}, Biel Obrador⁴ and Matthias Koschorreck¹



- Drawdown areas significantly contribute to areal extent to reservoirs
- Increasing trend with warming and droughts



Greenhouse gas emissions from drying streams and rivers

ARTICLES

<https://doi.org/10.1038/s41561-021-00734-z>

nature
geoscience

Check for updates

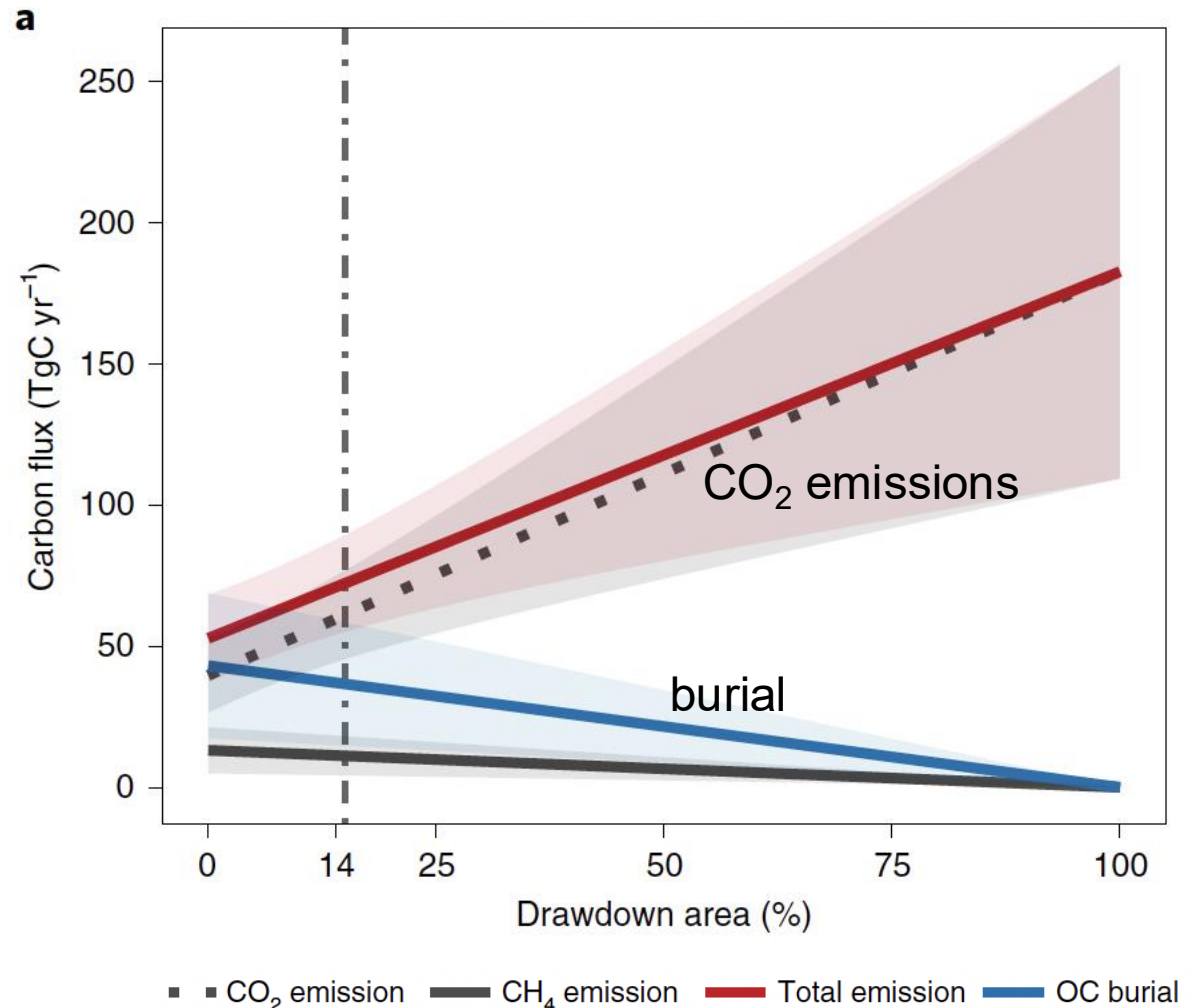
OPEN

Global carbon budget of reservoirs is overturned by the quantification of drawdown areas

Philippe S. Keller¹✉, Rafael Marcé^{2,3}, Biel Obrador⁴ and Matthias Koschorreck¹

OC burial in reservoirs decreases with drawdown area, CO_2 emissions increase

Therefore, elevated net loss flux of carbon with increasing drawdown area



Greenhouse gas emissions from drying streams and rivers

ARTICLES

<https://doi.org/10.1038/s41561-021-00734-z>

nature
geoscience

 Check for updates

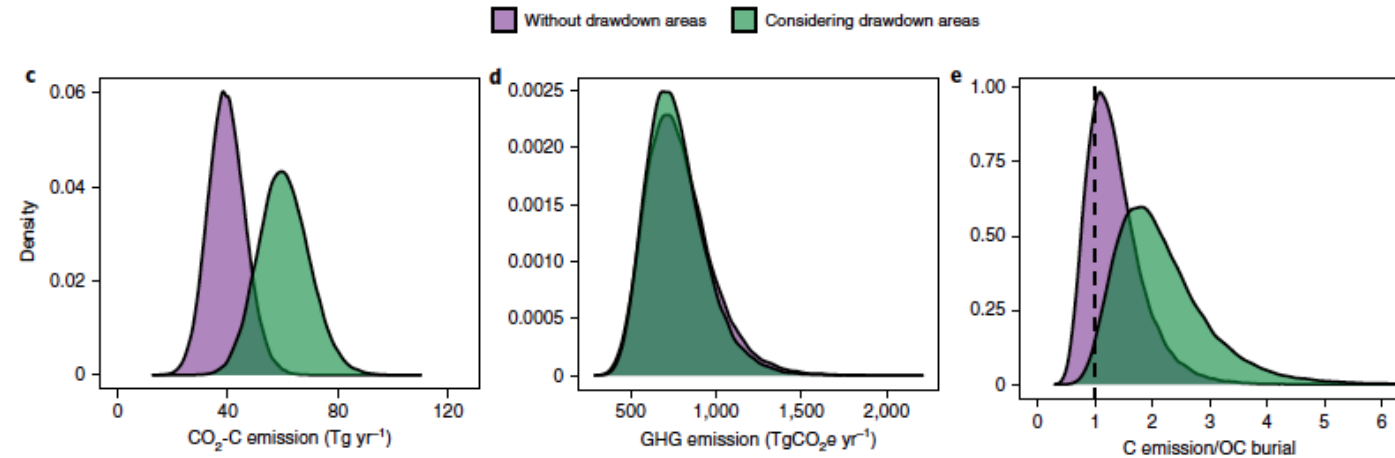
OPEN

Global carbon budget of reservoirs is overturned by the quantification of drawdown areas

Philippe S. Keller¹  Rafael Marcé^{2,3} Biel Obrador⁴ and Matthias Koschorreck¹ 

OC burial in reservoirs decreases with drawdown area, CO_2 emissions increase

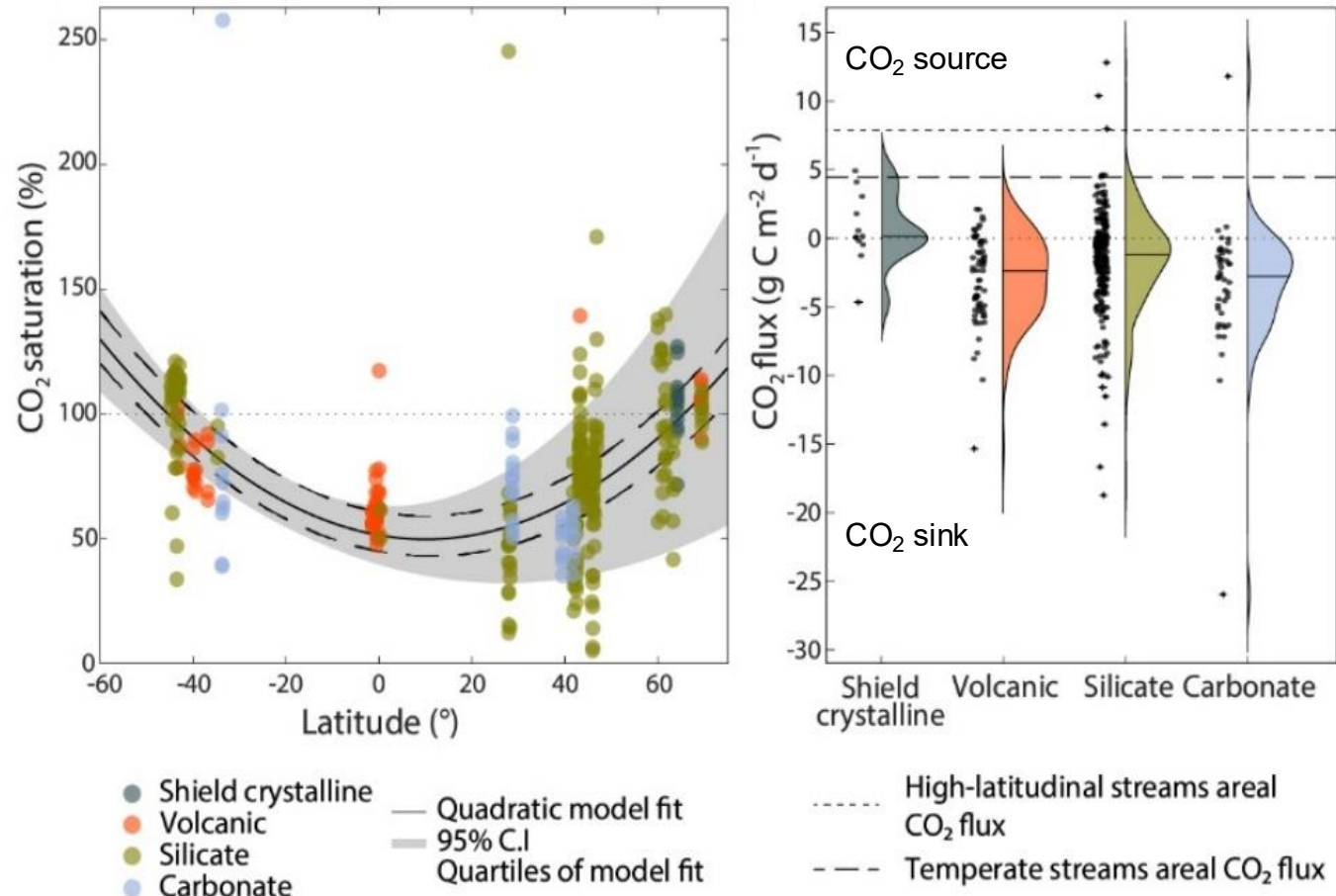
Therefore, elevated net loss flux of carbon with increasing drawdown area



Most streams are CO₂ emitters, but not all!

Glacier-fed streams and lakes

- Glacier-fed streams are CO_2 sinks depending on parent geology
- Chemical weathering consumes CO_2
- Likely in equilibrium with the atmosphere before industrialisation



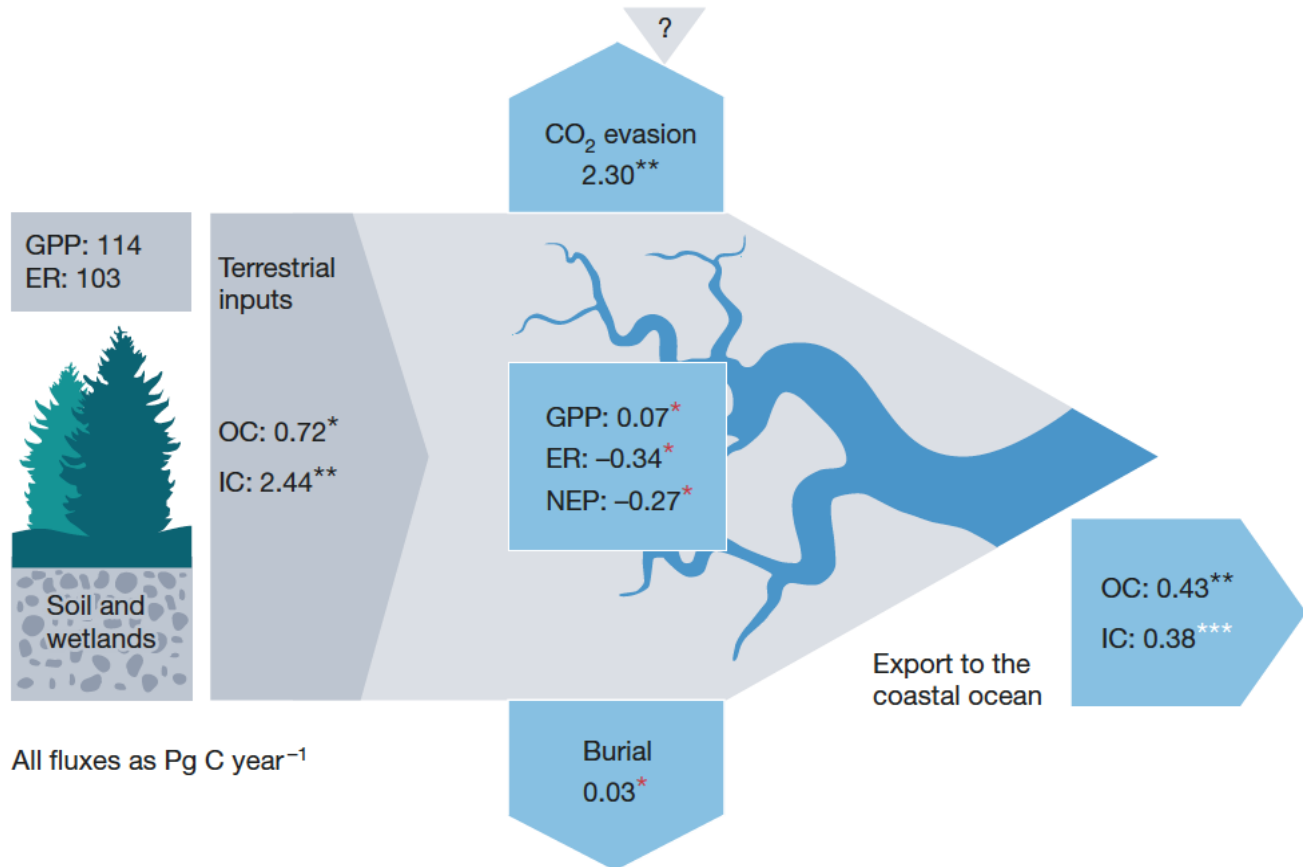
Streams and rivers are major components of the global

Review

River ecosystem metabolism and carbon biogeochemistry in a changing world

<https://doi.org/10.1038/s41586-022-05500-8>
Received: 12 March 2021
Accepted: 31 October 2022

Tom J. Battin^{1,2}, Ronny Lauerwald², Emily S. Bernhardt³, Enrico Bertuzzo⁴, Lluís Gómez Gener⁵, Robert O. Hall Jr.⁶, Erin R. Hotchkiss⁷, Taylor Maavaara⁸, Tamlin M. Pavelsky⁹, Lishan Ran^{10,11}, Peter Raymond¹², Judith A. Rosentreter^{12,13} & Pierre Regnier¹⁴



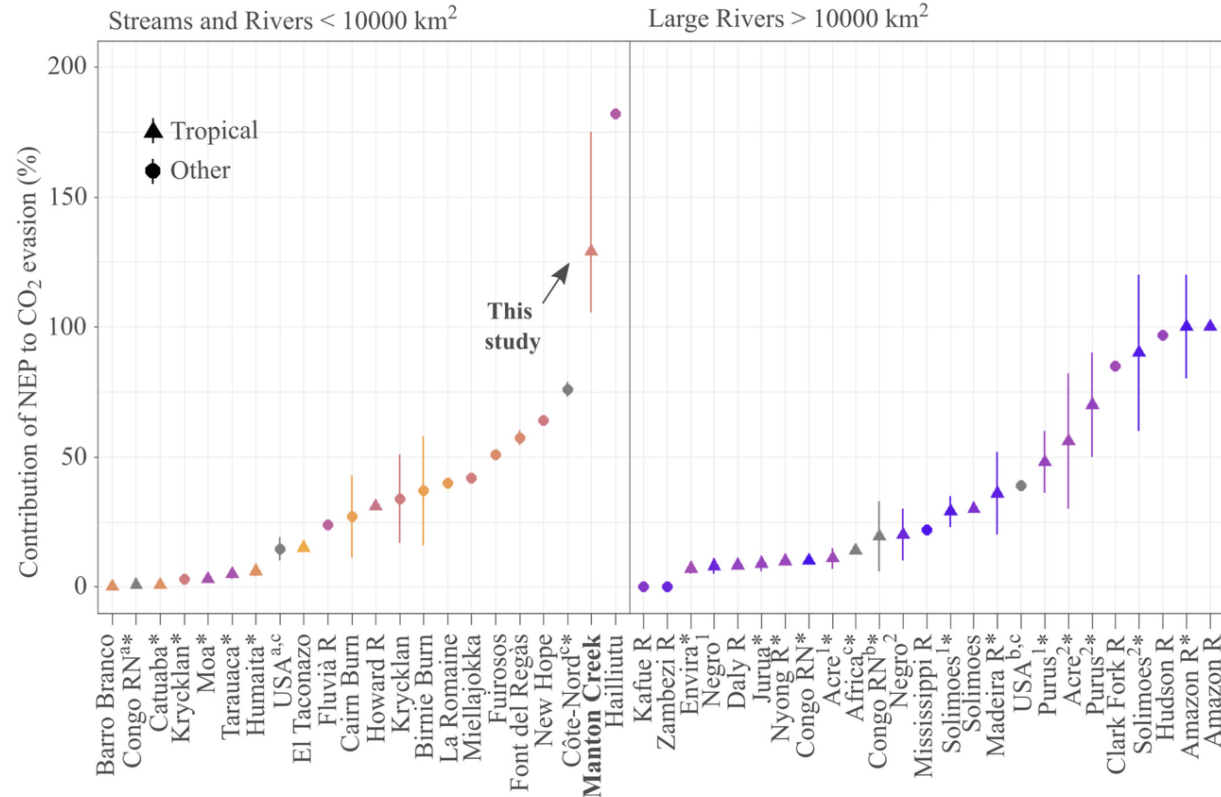
- CO₂ emissions from streams and rivers similar to the drawdown fluxes of atmospheric CO₂ by the world's oceans
- Ecosystem metabolism contributes ca. 10% to global CO₂ emissions – up to 90% locally.
- Remaining CO₂ from terrestrial primary production and chemical weathering

River networks matter for the global carbon cycle

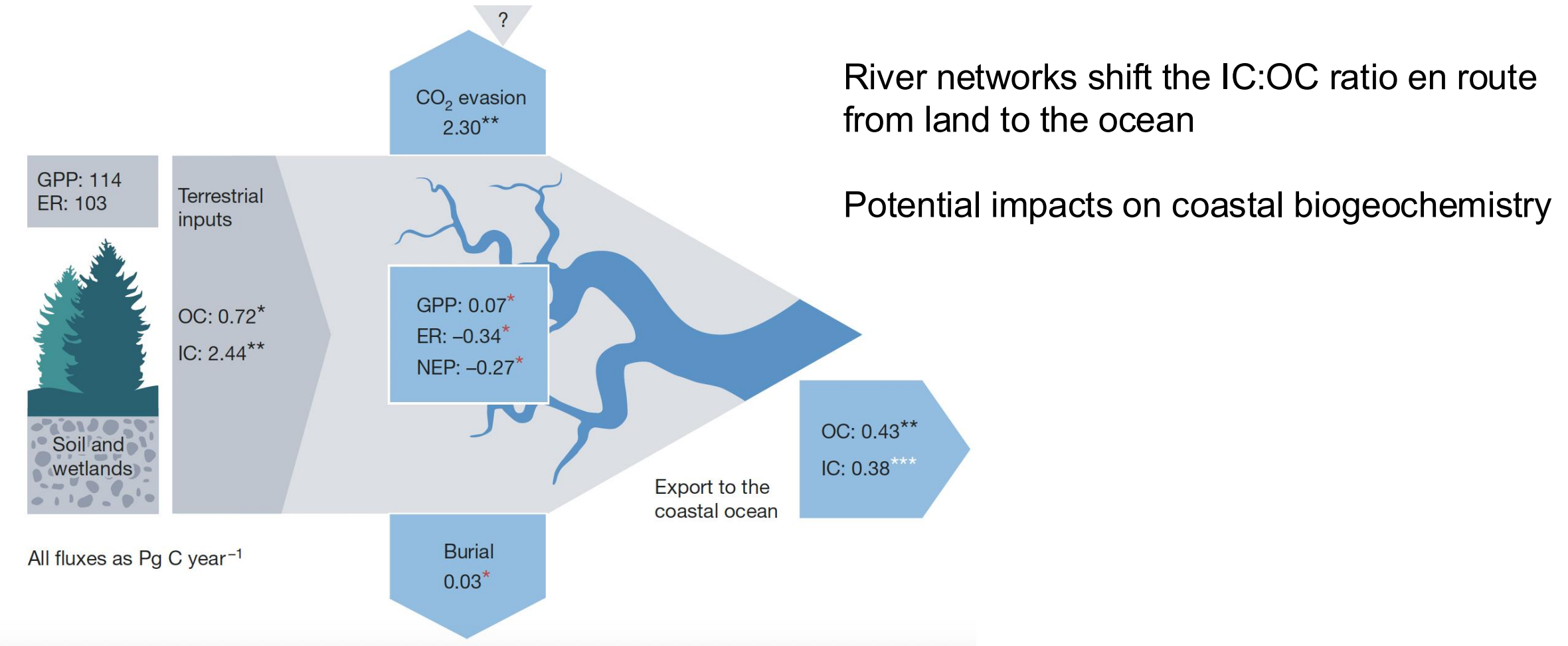
- Contributions from river NEP to CO₂ evasion from rivers vary widely
- Depend on gas exchange rate, carbonate dissolution, photochemistry etc

Stream respiration exceeds CO₂ evasion in a low-energy, oligotrophic tropical stream

Vanessa Solano  ^{1,*} Clément Duvert  ^{1,2*} Christian Birkel  ^{3,4} Damien T. Maher  ⁵ Erica A. García  ¹,
Lindsay B. Hulley  ¹



Streams and rivers are major components of the global carbon cycle



Stream and river networks

The multiple dimensions

Vertical

- Connected to the atmosphere through the turbulent surface
- Connected to the groundwater

Lateral

- Connected to groundwater, riparian zone and corridor

Longitudinal

- Ample opportunities for downstream processing (see RCC)

Network

- Small streams are most abundant and tightly connected to the terrestrial environment

Makes streams and rivers so important for carbon fluxes despite their minor contribution by areal extent